

Proteomic Profiling of *Bacillus subtilis* with Tylsoin

By

Jody Hawkes

Submitted in Partial Fulfillment of the Requirements

For the Degree of

Master's of Science

In the

Chemistry

Program

Youngstown State University

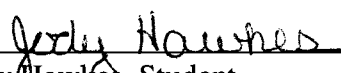
December, 2004

Proteomic Profiling of *Bacillus subtilis* with Tylosin


Jody Hawkes

I hereby release this thesis to the public. I understand that this thesis will be made available from the OhioLINK ETD Center and the Maag Library Circulation Desk for public access. I also authorize the University or other individuals to make copies of this thesis as needed for scholarly research.


Signature:

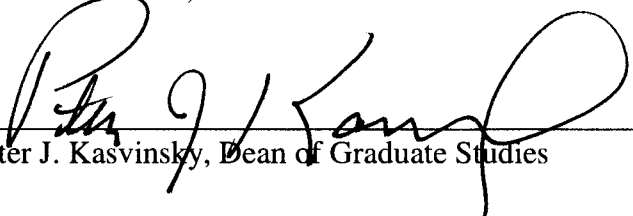
  
\_\_\_\_\_  
Jody Hawkes, Student 12-6-04  
Date

Approvals:

  
\_\_\_\_\_  
Dr. Thomas Kim, Thesis Advisor 12/6/04  
Date

  
\_\_\_\_\_  
Dr. Jeffrey Smiley, Committee Member 12/6/04  
Date

  
\_\_\_\_\_  
Dr. John Jackson, Committee Member 12/6/04  
Date

  
\_\_\_\_\_  
Peter J. Kasvinsky, Dean of Graduate Studies 12/7/04  
Date

## ABSTRACT

*Bacillus subtilis* is a Gram-positive bacterium capable of producing a wide range of industrially important enzymes and antibiotics; making it a perfect subject for proteomic-drug analysis. Here, *B. subtilis* will be grown with a minimum inhibitory concentration of the macrolide class antibiotic Tylosin, which inhibits protein synthesis. The results were compared to untreated *B. subtilis* control samples. Through two-dimensional gel analysis and digital imaging software, it is seen that acidic shifting occurred in the treated proteome expression profile indicating a chemical modification, via new isoelectric points, during the exposure of *B. subtilis* to Tylosin.

## Acknowledgements

I would first like to thank Youngstown State University for allowing me this opportunity to pursue a master's degree. I especially am very grateful to the Chemistry Department for everything that faculty and staff, especially Dr. Mincey have done for me over the years.

I would like to thank Dr. Tom Kim for being my advisor and for all his help in achieving this moment; also all of the members of the Proteomic Research Group, those present at Youngstown State and those now in other universities in lands far far away.

I would like to thank my family for supporting me, both financially and emotionally, through my quest of not only my master's degree but also my bachelor's degree as well; special recognition to my nephew Nikitas, for always having a way to cheer me up even on my worst days.

Last but not least, I would like to thank my husband Rob for putting up with me over the last two years and also supporting me in my journey. It has not been an easy one and I love that he has been there with me every step of the way.

## List of Abbreviations

2-D .....	Two-Dimensional
2-DE .....	Two-Dimensional Electrophoresis
IEF .....	Isoelectric Focusing
MIC .....	Minimum Inhibitory Concentration
PAGE.....	Polyacrylamide Gel Electrophoresis
PDF .....	Peptide Deformylase
pI .....	Isoelectric Point
SDS .....	Sodium Dodecyl Sulfate

## Table of Contents

Ch. 1: Introduction to <i>Bacillus subtilis</i> , Tylosin, Proteomics And Peptide Deformylase	1 - 12
1.1: Relevant Background of <i>Bacillus subtilis</i>	2 - 3
1.2: Results of Existing Proteomic Studies of <i>Bacillus subtilis</i>	3
1.3: Relevant Background of Tylosin	3 - 4
1.4: Relevant Background of Macrolides	4
1.5: Mechanistic Mode of Action for Tylosin	4 - 5
1.6: Relevant Background of Proteomics	6
1.7: Relevant Background of 2-DE	7 - 8
1.8: Advantages and Disadvantages of 2-DE	8
1.9: Relevant Background of Peptide Deformylase	8 - 9
1.10 Current Proteomic Studies Involving PDF	9 - 10
1.11 References	11 - 12
Ch. 2: Materials and Methods	29 - 33
2.1: Bacterial Growth Preparations	30
2.2: MIC Determination	30 - 31
2.3: Modified Bradford Assay	31
2.4: Two-Dimensional Electrophoresis	31 - 32
2.5: Imaging	32
2.6: References	33

Ch. 3: Results and Discussion	34 - 42
3.1: Results of MIC Determination	35
3.2: Results of Modified Bradford Assay	35
3.3: Results of Treated Match Set	36
3.4: Results of Untreated Match Set	37
3.5: Results of Higher Level Match Set	38
3.6: Discussion	38 - 41
3.7: References	42

## Tables and Figures

Table 1.1: General Features of the <i>Bacillus subtilis</i> Genome	14
Figure 1.1: Structure of Tylosin	16
Figure 1.2: Structure of Erythromycin	18
Figure 1.3: Secondary-Structure Model of the Peptidyl Transferase Center in Domain V of 23S rRNA	20
Figure 1.4: Secondary-Structure Model of Hairpin 35 in Domain II	22
Figure 1.5: Types of Proteomics and their Applications	24
Figure 1.6: Treatment of <i>Bacillus subtilis</i> (A) and Actinonin (B)	26
Figure 1.7: Treatment of <i>H. influenzae</i> (A) with Actinonin (B)	28
Figure 3.1: Growth Curve of <i>Bacillus subtilis</i> with Tylosin	44
Figure 3.2: Absorbance vs Concentration for <i>Bacillus subtilis</i> 5.84 mg/mL And Tylosin-Treated <i>Bacillus subtilis</i> 4.01 mg/mL Protein Samples	46
Figure 3.3: Absorbance vs Concentration for <i>Bacillus subtilis</i> 5.73 mg/mL, 6.94 mg/mL and Tylosin-Treated <i>Bacillus subtilis</i> 9.12 mg/mL, 12.61 mg/mL Protein Samples	48
Figure 3.4: Tylosin-Treated <i>Bacillus subtilis</i> Uncropped 4.01 mg/mL Gel Image	50
Figure 3.5: Tylosin-Treated <i>Bacillus subtilis</i> Match Set	52
Figure 3.6: Tylosin-Treated <i>Bacillus subtilis</i> Match Set with Protein Spot Comparisons	54



Table 3.1: Summary of Tylosin-Treated Match Set	56
Figure 3.7: Untreated <i>Bacillus subtilis</i> Uncropped 5.73 mg/mL Gel Image	58
Figure 3.8: Untreated <i>Bacillus subtilis</i> Match Set	60
Figure 3.9: Untreated <i>Bacillus subtilis</i> Match Set with Protein Spot Comparisons	62
Table 3.2: Untreated <i>Bacillus subtilis</i> Match Set Summary	64
Figure 3.10: Higher Level Match Set Featuring the Master Gel Images of the Treated and Untreated <i>Bacillus subtilis</i> Match Set	66
Figure 3.11: Higher Level Match Set with Protein Spot Comparisons	68

## Appendix

Appendix I: Solutions for Experiments

70

## **Chapter 1**

Introduction to *Bacillus subtilis*, Tylosin, Proteomics, and Peptide Deformylase

### **Section 1.1: Relevant Background of *Bacillus subtilis*:**

Members of the genus *Bacillus* are Gram-positive, endospore forming, rod-shaped bacteria that grow aerobically (1). At present, there are sixty-five described species in the *Bacillus* genus; mainly separated into five different groups based on 16S rRNA sequence analysis (2).

Scientific interest in *B. subtilis* was first sparked by the opportunity to investigate the developmental system of sporulation. It then gained popularity in the bacterium's ability to synthesize and secrete exceptional amounts of industrially important enzymes and antibiotics. Two-thirds of the United States world markets of industrial enzymes are produced by the *Bacillus* species with an estimated net worth of \$800 million. *Bacillus* species are also famous for producing a wide variety of secondary metabolites with antimetabolic and pharmacological activities (1).

Members of the genus *Bacillus* are frequently used as hosts for the production of biomedical recombinant proteins such as pro-insulin and staphylokinase. Table 1.1 summarizes the general features of the *B. subtilis* genome. Most notable is the 4,214,810 base pairs present in the *B. subtilis* (2). The corresponding *B. subtilis* two-dimensional (2-D) protein index (Sub2D at <http://microbio2.biologie.uni-greifswald.de>: 8880) currently contains roughly two hundred entries.

In addition to a large number of proteins with still unknown functions, the known proteins can be allocated into two groups: (1) proteins synthesized particularly during cell growth which fulfill mainly house keeping functions such as glycolysis, tricarboxylic acid cycle, amino acid biosynthesis and (2) proteins produced particularly in growth-arrested cells in response to stress and starvation which may have a specific or more

general protective function against stress or starvation in the non- or slow- growing cells (3).

### **Section 1.2: Results of Existing Proteomic Studies of *Bacillus subtilis*:**

Because of their relatively low complexity, bacterial cells are exceptionally well-suited model systems for the description of the entire proteome of an organism. Proteomic studies previously published by Büttner and his group demonstrated that approximately two-thirds of the protein spots are located in the neutral or weakly acidic region and the remaining third in the more alkaline region (4).

The analysis of the theoretical proteome of *B. subtilis* also revealed that most of the proteins with more than two membrane-spanning domains are located in the alkaline region. No intrinsic membrane proteins have ever been found. Strongly hydrophobic proteins are preferentially lost during the 2-D gel electrophoresis and were not detected. Multiple spots can be attributed either to post-translational modifications or to artificial chemical modifications occurring during protein preparation; they may have new isoelectric point (pI) values (4).

Ohimier and his group demonstrated that with classical 2-D electrophoresis, alkaline proteins were normally lost by cathodic drift of carrier ampholyte focusing (5).

### **Section 1.3: Relevant Background of Tylosin:**

Tylosin, brand name Tylan, is produced by the actinomycete *Streptomyces fradiae*. Tylosin has been widely used as a feed additive for the promotion of animal growth and

remains in common veterinary use against bacterial dysentery and respiratory diseases in poultry, swine, and cattle (6).

Tylosin belongs to the antibiotic class known as macrolides. Macrolides are named based on their chemical structure which consists of a large lactone ring attached to a number of sugars (7). Clinically useful macrolides consists of a 14-15-16 member lactone ring; Tylosin is a 16-membered ring (figure 1.1) (8).

#### **Section 1.4: Relevant Background of Macrolides:**

These drugs are potent inhibitors of protein biosynthesis and bind to the larger 50S ribosomal subunit and prevent the translocation step of translation. These compounds also prevent the assembly of the 50S particle in cells, without interfering with the 30S subunit biosynthesis (9).

The macrolides are lipid soluble and diffuse readily into intracellular tissues. They are classified as “time dependent”, implying that plasma should exceed the minimum inhibitory concentration (MIC) of the infecting organism for the majority of the dosing interval. Organisms are considered susceptible at an MIC of less than  $2 \mu\text{g}\cdot\text{mL}^{-1}$  (6).

#### **Section 1.5: Mechanistic Mode of Action for Tylosin:**

Tylosin has a similar mechanistic mode of action as its class mate erythromycin which is a 14-membered lactone ring (figure 1.2) with different sugar side chains (9). The inhibitory action of erythromycin is effected at the early stages of protein synthesis when the drug blocks the growth of the nascent peptide chain, presumably causing premature association of the peptidyl-tRNA from the ribosomal subunit (8).

The macrolide binding site is most likely situated at the base of the deep cleft that provides access to the peptide exit channel of the large subunit. This is at, or very close to, the location where the aminoacyl and peptidyl ends of the tRNA's become aligned within the large subunit to catalyze the formation of peptide bonds. The site of peptide bond formation on the large ribosomal subunit (the peptidyl transferase center) is coupled with the central loop in domain V of the 23S rRNA (figure 1.3) (8). The peptide transferase center catalyzes the formation of peptide bonds, linking amino acids to the growing polypeptide chains during the synthesis of new proteins (10). The interaction sites of erythromycin have additionally been mapped to hairpin 35 in domain II (figure 1.4) of the rRNA. A single molecule of erythromycin binds per large ribosomal subunit indicating that the same drug molecule simultaneously contacts domain II and V of 23S rRNA. As these drugs are small relative to the ribosome, such interactions would be possible only if the rRNA is folded so that hairpin 35 and the peptidyl transferase loop are adjacent.

Most recent evidence indicates that the 16-membered ring of the macrolide tylosin also interacts with the peptidyl transferase and the hairpin 35 loop. Two resistance determinants, *tlrA* and *tlrB* encode another type of methyltransferase that methylates G748 in the hairpin 35 loop. The structure of the drug binding pocket within the large ribosomal subunit is defined by the tertiary configuration of 23S rRNA. Hairpin 35 and the peptidyl transferase loop seem to be the main, although not the sole, components of this binding pocket. Nucleotide 2032 within the loop of 23S rRNA hairpin 72 is also implicated (8).

## **Section 1.6: Relevant Background of Proteomics:**

The term “proteomics” was coined in 1995. Figure 1.5 summarizes the aspects of proteomics and some of their applications. Proteomics is the study of the proteome. A proteome refers to the entire protein complement expressed by a genome. Proteome analysis supplements gene sequence data with protein information about where and in which ratio and under what conditions proteins are expressed. A proteome is like a snapshot of a physiological scenario. Proteomics and genomics are complementary. Genomics has fundamental restrictions that gene sequence data contains insufficient information to understand the function of gene products (11).

The connection between the dynamic expression of a proteome and the physiological changes related to a healthy or diseased condition can help to support the understanding of disease mechanisms, design new ways for the discovery and validation of disease models, find new diagnostic markers, identify potential therapeutic targets, optimize lead compounds for clinical development, characterize drug effects, and study protein toxicology (11). Cancer, heart disease, inflammatory, and autoimmune diseases are prime areas for proteomic studies (12).

The basic laboratory protocol of Proteomics is solubilization of proteins from the sample, separation of protein by two-dimensional electrophoresis (2-DE), digitization of 2-D gels and computer-assisted analysis of protein spot patterns, determination of specific attributes of the proteins of interest by mass spectrometry, and searching databases with the hopes of identifying the proteins (13).



### **Section 1.7: Relevant Background of 2-DE:**

In 1975, two-dimensional polyacrylamide gel electrophoresis (2-D PAGE) was introduced as a method to separate complex mixtures of cellular protein into individual polypeptides. The underlying concept is to find proteins that respond specifically and uniquely to particular states of the cell. Each set of proteins, termed a proteomic signature, relates to the current working status of a particular core metabolic process. The physiological state of the cell in a particular circumstance is read from the ensemble of the proteomic signatures displayed (14).

The high resolution capability of 2-DE stems from the fact that the first and second dimensions are based on two independent protein characteristics. The first dimension, of 2-DE is isoelectric focusing (IEF), during which the proteins are separated based on their charge. In the second dimension, the proteins are separated orthogonally by sodium dodecyl sulfate polyacrylamide gel electrophoresis (SDS-PAGE) according to their molecular weight (13).

2-DE is used in expression proteomics in which protein profiles are compared quantitatively and qualitatively between any given sample pair. The appearance and disappearance of protein spots tell the difference of protein expression while the varied intensity of the spots reflects the different protein expression levels under a given condition. 2-DE protein profiling is especially useful in biomarker discovery in which comparison can be made between normal and diseased samples. 2-DE also features great strength of separating protein isoforms resulting from protein posttranslational modifications, alternative mRNA splicing and proteolytic processing due to a disease condition or drug treatment. These kinds of protein modifications and cellular processing

change the molecular mass and the pI of proteins, leading to the appearance of different spots in 2-D gels (12).

### **Section 1.8: Advantages and Disadvantages of 2-DE:**

2-DE has several advantages: the information content of data obtained by the 2-DE based approach is high because a number of specific protein attributes can be determined. Thousands of proteins can be resolved and visualized simultaneously on a single 2-DE gel. High resolution capabilities of 2-DE allow the separation and detection of post translational modified proteins. Individual steps of the proteome analysis (2-DE, imaging, mass spectrometry, database searching) can be separated in space and time.

2-DE also has several limitations: protein expression in a biological system changes with the state of development, in response to environmental stimuli, with the progression of disease, etc. different cells within a multicellular organism have different proteomes. The dynamic range of protein expression spans seven or eight orders of magnitude and consequently proteins are present in vastly different quantities. Furthermore, proteins within a proteome are structurally diverse and have various physiochemical characteristics. It is also not possible to analyze the entire proteome. Proteins displayed in a single 2-DE gel represent only a portion of all the proteins that are present in a sample. 2-DE is labor intensive and has a relatively low throughput (13).

### **Section 1.9: Relevant Background of Peptide Deformylase:**

Peptide Deformylase (PDF) is essential in a variety of pathogenic bacteria but is not required for cytoplasmic protein synthesis in eukaryotes and is therefore an interesting

potential target for antibacterial agents. Protein synthesis in eubacteria, under normal conditions, is initiated by formyl-methionyl-tRNA. Consequently, all nascent polypeptides are synthesized with N-formyl-methionine at the N-terminus. The formyl group is removed by PDF during elongation of the polypeptide chain. As methionine aminopeptidase cannot hydrolyze N-blocked polypeptides, deformylation is also a prerequisite for protein maturation (15).

*B. subtilis* possesses two functional PDF's YkrB and Def. YkrB is the major PDF; however, single deletion mutants in both genes are viable indicating that the two enzymes can be at least partially substituted for each other (16).

#### **Section 1.10: Current Proteomic Studies Involving PDF:**

The Def protein is essential for bacterial survival and has been identified in all eubacteria except in *Archaea*, *Saccharomyces cerevisiae*, and *Caenorhabditis elegans*. Actinonin is active against both Gram-positive and Gram-negative bacteria indicating a high degree of similarity among eubacterial deformylases making it a wonderful drug target (17).

Prior proteomic studies of the protein synthesis pattern of wild-type *B. subtilis* changed upon treatment with actinonin (figure 1.6). After just ten minutes, most of the newly synthesized protein spots had shifted to a lower pI compared to protein spots in an untreated control (16).

Another study involving the Gram-positive bacteria *Haemophilus influenza* and actinonin yielded similar results (figure 1.7). Little change was observed for the high molecular weight proteins while the pI's of the majority of the low molecular weight

proteins were changed. It was concluded, in all cases, that the pI shifts were do to the formyl groups not being removed and blocking the N-terminal amino groups (15).

### **Section 1.10: References:**

- (1). Devine, K., The *Bacillus subtilis* Genome Project: Aims and Progress. *TIBTECH*. **1995**, 13, 210-216.
- (2). Tosato, V.; Bruschi, C.V. Knowledge of the *Bacillus subtilis* Genome: Impacts on Fundamental Science and Biotechnology. *Appl Microbiol Biotechnol*. **2004**, 64, 1-6.
- (3). Bernhardt, J.; Büttner, K.; Scharf, C. Dual Channel Imaging of Two-Dimensional Electropherograms in *Bacillus subtilis*. *Electrophoresis*. **1999**, 20, 2225-2240.
- (4). Büttner, K.; Bernhardt, J.; Scharf, C.; etc. A Comprehensive Two-Dimensional Map of Cytosolic Proteins of *Bacillus subtilis*. *Electrophoresis*. **2001**, 22, 2908-2935.
- (5). Ohimeier, S.; Scharf, C.; Hecker, M. Alkaline Proteins of *Bacillus subtilis*: First Steps Towards a Two-Dimensional Alkaline Master Gel. *Electrophoresis*. **2000**, 21, 3701-3709.
- (6). Liu, M.; Douthwaite, S. Resistance to the Macrolide Antibiotic Tylosin is Conferred by Single Methylations at 23S rRNA Nucleotides G748 and A2058 Acting in Synergy. *PNAS*. **2002**, 99, 14658-14663.
- (7). Noli, C.; Boothe, D. Macrolides and Licosamides. *Veterinary Dermatology*. **1999**, 10, 217- 223.
- (8). Vester, B.; Douthwaite, S. Macrolide Resistance Conferred by Base Substitutions in 23S rRNA. *Antimicrob. Agents Chemother*. **2001**, 45, 1-12.

- (9). Champney, S.W.; Tober, C.L. Specific Inhibition of 50S Ribosomal Subunit Formation in *Staphyococcus Aureus* Cells by 16-Membered Macrolide, Lincosamide, and Streptogramin B Antibiotics. *Current Microbiology*. **2000**, 41, 126-135.
- (10). Douthwaite, S. Structure Activity Relationships of Ketolides vs Macrolides. *CMI*. **2001**, 7, 11-17.
- (11). Kellner, R. Proteomics: Concepts and Perspectives. *Fresenius J Anal Chem*. **2000**, 366, 517-524.
- (12). He, Q.; Chiu, j. Proteomics in Biomarker Discovery and Drug Development. *J. Cell. Biochem*. **2003**, 89, 868-886.
- (13). Beranova-Giorgianni, S. Proteome Analysis by Two-Dimensional Gel Electrophoresis and Mass Spectrometry: Strengths and Limitations. *Trends Anal. Chem*. **2003**, 22, 273- 281.
- (14). VanBogelen, R.; Schiller, E.; Thomas, J. Diagnosis of Cellular States of Microbial Organisms Using Proteomics. *Electrophoresis*. **1999**, 20, 2149-2159.
- (15). Apfel, C.; Locher, H.; Evers, S.; etc. Peptide Deformylase as an Antibacterial Drug Target: Target Validation and Resistance Development. *Antimicrob. Agents Chemother*. **2001**, 45, 1058-1064.
- (16). Bandow, J.; Freiberg, C.; Hecker, M.; etc. The Role of Peptide Deformylase in Protein Biosynthesis: A Proteomic Study. *Proteomics*. **2003**, 3, 299-306.
- (17). Haas, M.; Beyer, D.; Gahlmann, R.; etc. YkrB is the Main Peptide Deformylase in *Bacillus subtilis*, a Eubacterium Containing Two Functional Peptide Deformylase. *Microbiology*. **2001**, 147, 1783-1791.

**Table 1.1**

General Features of the *Bacillus subtilis* genome

Moszer, I. The complete Genome of *Bacillus subtilis*: From Sequence Annotation to Data Management and Analysis. *FEBS Letters*. **1998**, 430, 28-36.

**Genome size** 4,914,914 bp (*oriC*: 0 kb, *oriS*: 2,017 kb)  
**European sequencing** 2,677 kb (54%)  
**Japanese sequencing** 1,925 kb (39%)  
 (17 kb overlap)  
**Functional sequencing** 106 kb (4%)

**Base composition (%)**

	Genome	Leading strand	Protein genes	RNA genes	Intergenic regions	Prophages
A	26.3	29.4	29.9	29.0	31.1	30.8
C	21.8	20.1	20.5	20.6	19.9	19.2
G	21.7	20.6	24.1	21.4	18.6	18.1
T	29.3	27.9	25.7	29.1	31.5	31.9

=> whole genome: 48.6% G+C

**Gene counts**

**Protein genes** 4,160 (2,269 *y* genes, see similarities in Table 2)  
**rRNAs** 10 operons (18S-23S-5E)  
**tRNAs** 69 (13 operons, 8 single genes)  
**Other small RNAs** 3 (106, 4.0E, RNase P)

**Coding capacity (kb)**

**Protein genes** 3,440.3 (80.6%)  
**Stable RNAs** 63.6 (1.6%)  
 => overall coding 3,700.0 (87.8%)  
**Intergenic regions** 514.8 (13.2%)

**Orientation of transcription (CDS)**

	Clockwise	Leading strand
+	1,387 (47.2%)	3,820 (78.9%)
-	2,109 (52.8%)	1,079 (106.1%)

**Lengths (bp)**

	Mean	Min	Max
Protein genes	824	48	14,760
Intergenic regions	127	<0	3,191

=> density: 1 gene / 1.09 kb

**Start and stop codons**

	Start	Stop
ATG	3,185 (77.7%)	TAA 2,545 (82.1%)
TTG	813 (19.5%)	TGA 964 (29.5%)
GTG	227 (5.4%)	TAG 691 (14.4%)
CTG	8 (0.2%)	
ATT	6 (0.1%)	

**Codon usage (CDS)**

**Class 1** 3,070  
**Class 2 (high expression)** 100  
**Class 3 (prophages)** 87

**Prophage(s)-like regions**

Name	Coordinates (bp)	Length (kb)
1	302,603-325,080	23
2	329,603-370,080	41
3	332,603-354,080	22.5
4	1,303,603-1,379,080	76
PBEK	1,308,603-1,348,080	25
5	1,379,603-1,400,080	21
6	2,046,003-2,076,080	32
EPK	2,164,274-2,266,080	134.416
<i>shin</i>	2,852,698-2,910,085	48.088
7	3,707,603-3,750,080	43

=> 9.5% of the genome

**Non-stably repeated DNA sequences longer than 100 bp (RNA, *orf*, *phi*, *psi* and prophage genes excluded)**

Length (bp)	Coordinates (bp)	Genes
748	2,854,918 and 2,871,347	<i>gins</i> and <i>top2</i>
410	4,101,819 and 4,102,329	<i>yzxL</i> and <i>yzxK</i>
87	4,186,668 and 4,186,740	<i>ypcO</i> and <i>ypcL</i>
174	688,346 and 688,520	<i>yafI</i>
118	4,088,843 and 4,088,960	<i>yafB</i> and <i>yafC</i>

See positions of the 100 bp non-coding element in Figure 2



**Figure 1.1**

Structure of Tylosin

Sigma-Aldrich. <http://www.sigmaaldrich.com> (accessed Nov 2004)

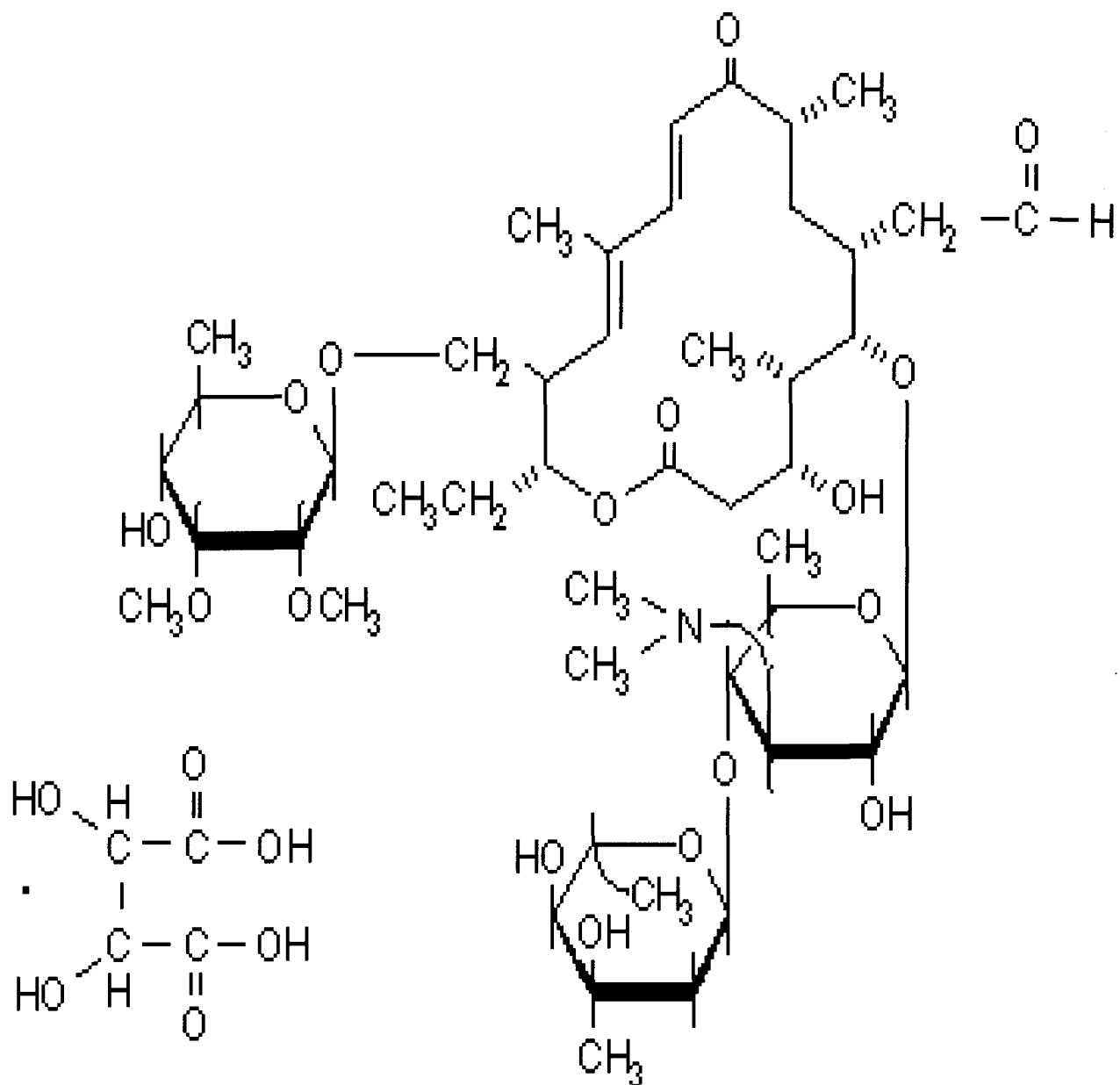


**Figure 1.2**

Structure of Erythromycin

Sigma-Aldrich. <http://www.sigmaaldrich.com> (accessed Nov 2004)

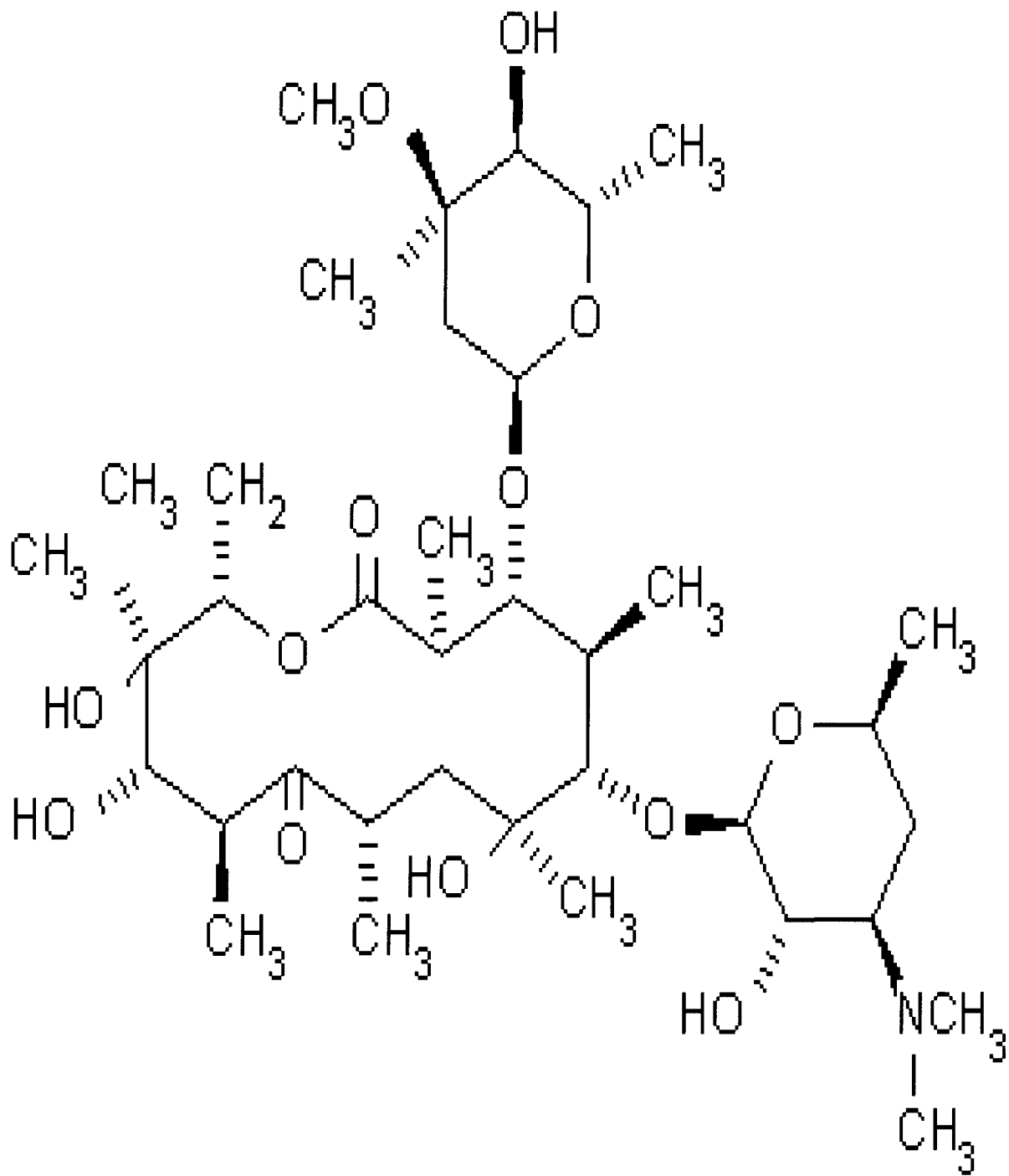


**Figure 1.3**

Secondary-Structure Model of the Peptidyl Transferase Center in Domain V of 23S  
rRNA

Vester, B.; Douthwaite, S. Macrolide Resistance Conferred by Base Substitutions in 23S  
rRNA.

*Antimicrob.AgentsChemother.* **2001**, 45, 1-12.

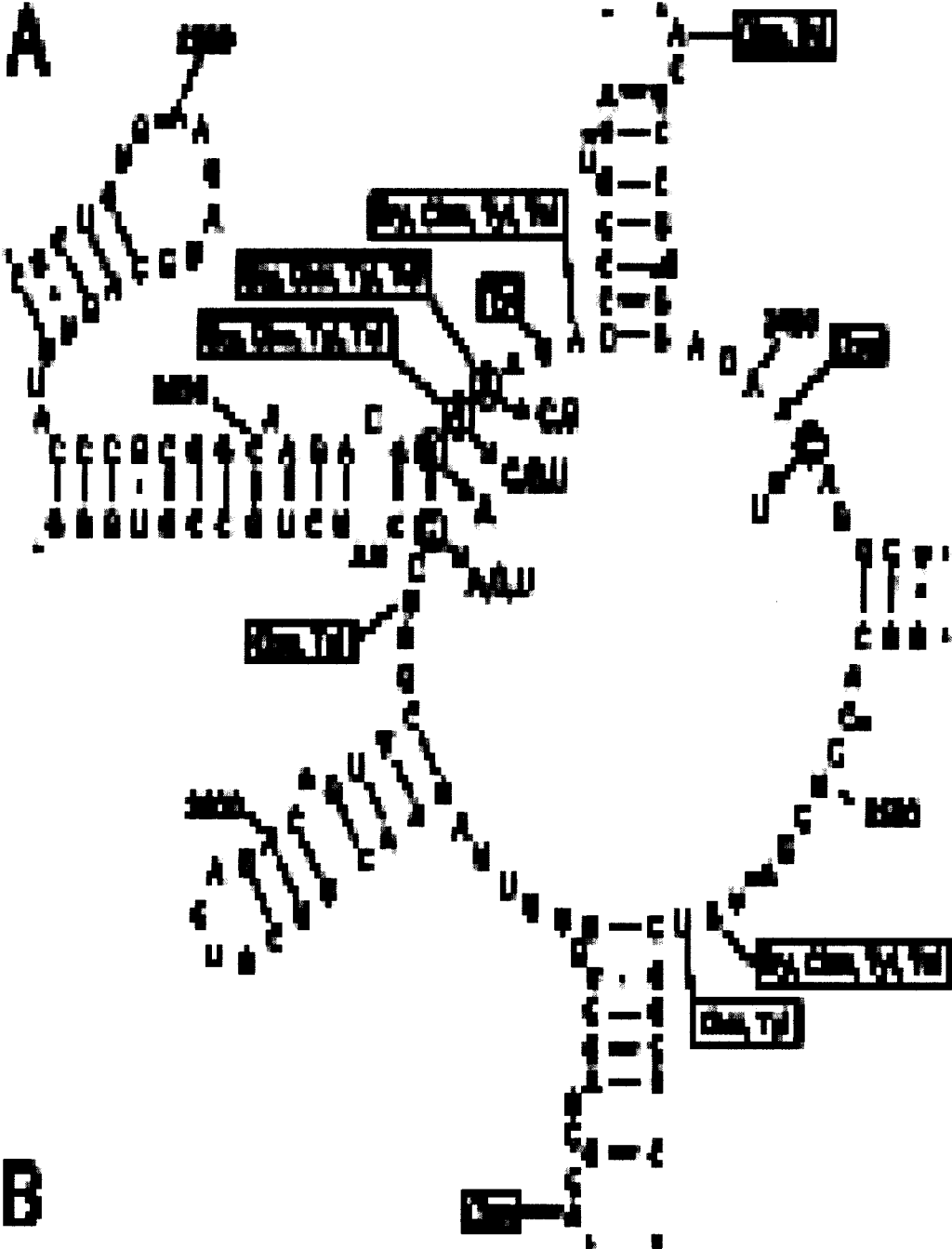


**Figure 1.4**

Secondary-Structure Model of Hairpin 35 in Domain II

Vester, B.; Douthwaite, S. Macrolide Resistance Conferred by Base Substitutions in 23S rRNA.

*Antimicrob. Agents Chemother.* **2001**, 45, 1-12.





**Figure 1.5**

Types of Proteomics and their Applications

Graves, P.; Haystead, T. Molecular Biologist's Guide to Proteomics. *Miorobiol. Mol.*

*Biol. Rev.* **2002**, 66, 39-63.

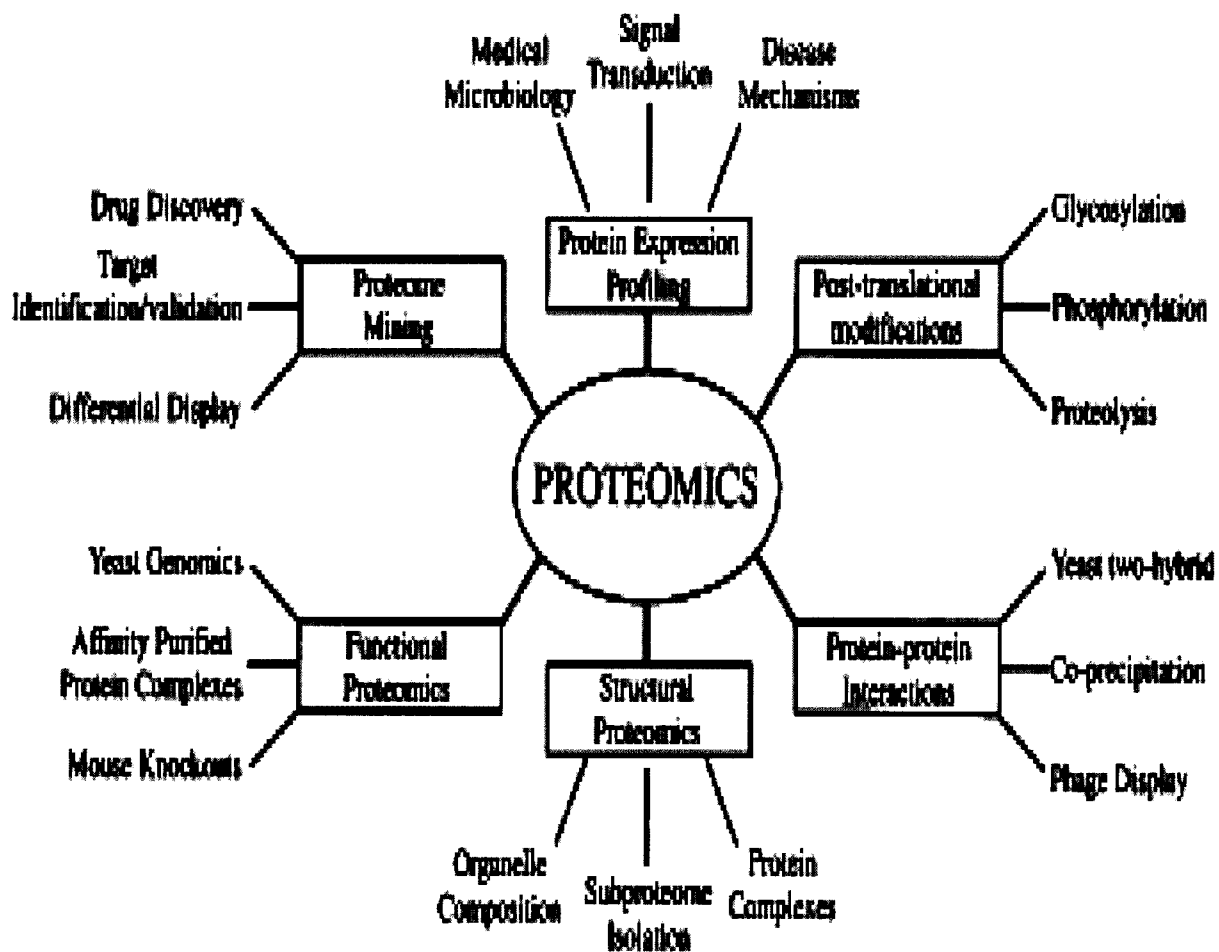


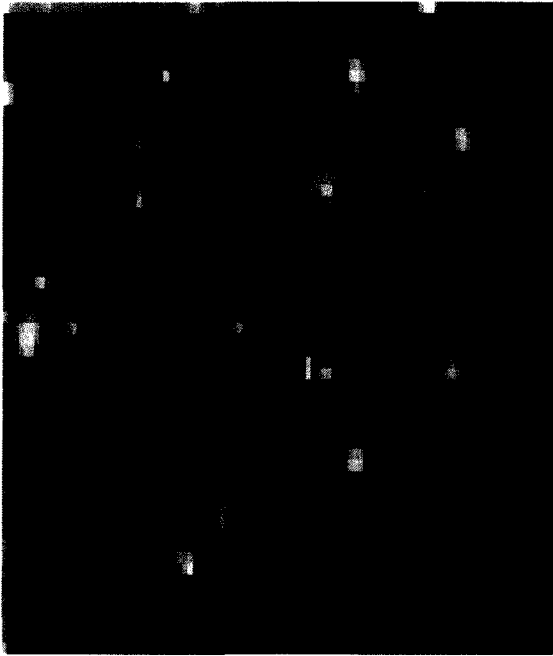
**Figure 1.6**

Treatment of *Bacillus subtilis* (A) with Actinonin (B)

Bandow, J.; Labischinski, H.; Hecker, M.; etc. Proteomic Approach to Understanding Antibiotic Action. *Antimicrob. Agents Chemother.* **2003**, 47,948-955.

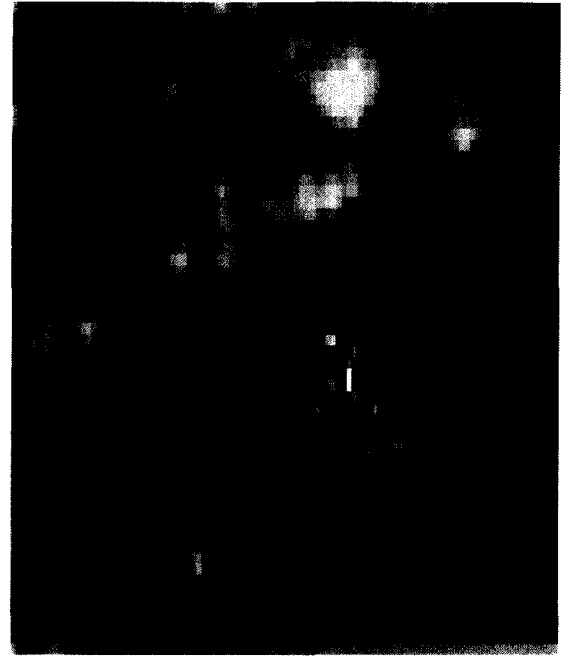
**A**

**basic**



**B**

**acidic basic**



**acidic**

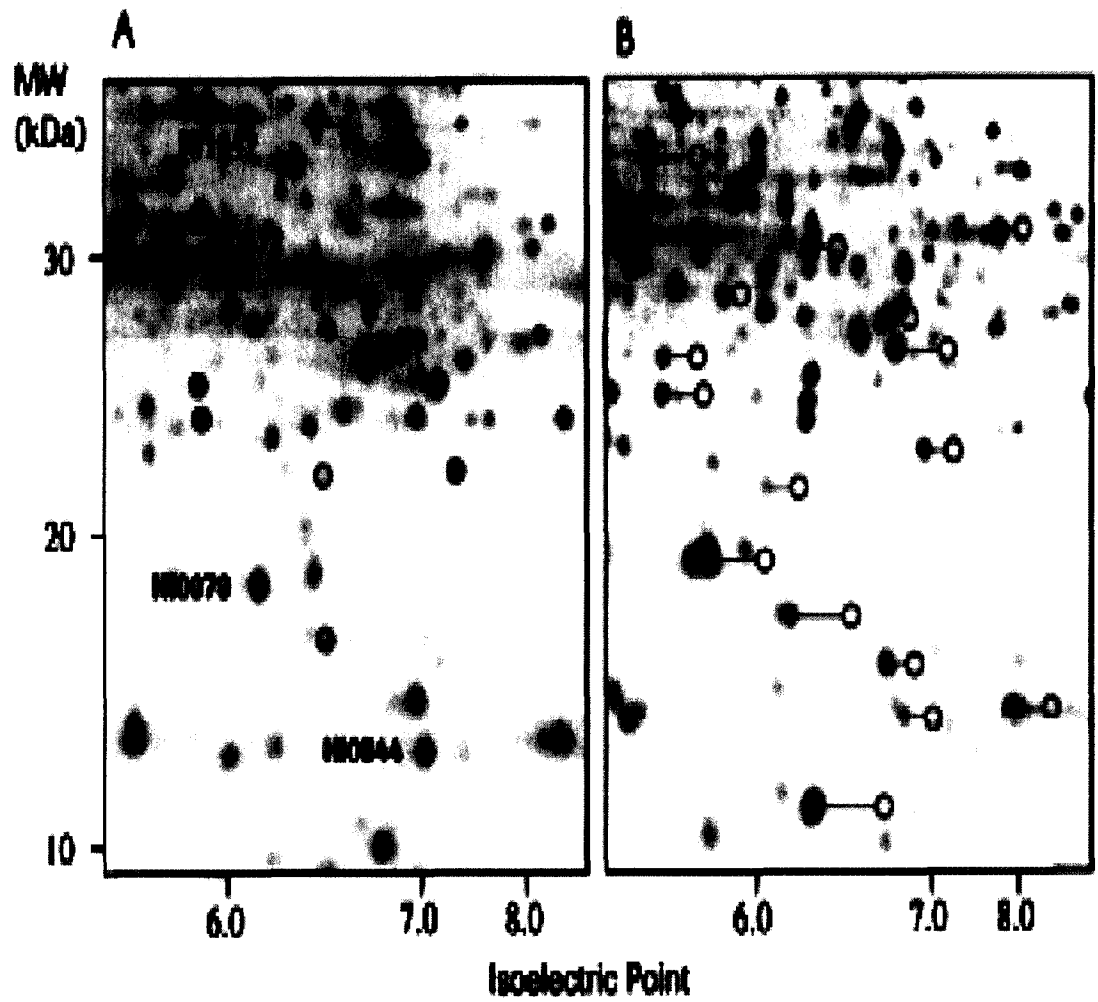
**Figure 1.7**

Treatment of *H. influenzae* (A) with Actinonin (B)

Apfel, C.; Locher, H.; Evers, S.; etc. Peptide Deformylase as an Antibacterial Drug

Target: Target Validation and Resistance Development. *Antimicrob. Agents Chemother.*

**2001**, 45, 1058-1064



## **Chapter 2**

### Materials and Methods

### **Section 2.1: Bacterial Growth Preparation:**

*Bacillus subtilis* (strain 6051-T; ATCC) was grown in a sterile flask containing sterile Luria-Bertani (LB) broth. The broth contained bacto tryptone, bacto yeast extract, and sodium chloride. The flask was placed in a 25°C Lab-Line Orbit Environ-Shaker for forty-eight hours. The resulting cell culture was collected in two 50mL conical centrifuge tubes at roughly 40 mL apiece. The tubes were placed in a Beckman GPR Centrifuge and spun at 5,000 rpm at 4°C for twenty minutes. Bacterial pellets were washed, three times, with TE buffer, pH 7.5, (10 mM Tris, 1 mM EDTA) and centrifuged. The supernatant was then decanted and the resulting pellet was weighed. For each pellet weighed, 200 µL of 2-DE buffer (8.4 M Urea, 2.4 M Thiourea, 5% CHAPS, 50 mM DTT, 25 mM Spermine Base) per 50 mg was added. The resulting mixture was sonicated via a Fischer Sonic Dismembrator in thirty second cycles at 60 Hz with cooling on ice for another thirty seconds and repeated a total of three times. Upon completion, the sample was centrifuged at 16,400 rpm at 4°C for thirty minutes. The resulting supernatant was collected and frozen for future use.

### **Section 2.2: MIC Determination:**

In the determination of the minimum inhibitory concentration (MIC), 80 µL of Tylosin (8 mg/mL total sample concentration) was added to 10 mL of sterile LB broth and serially diluted ( $2.0 \times 10^{-6}$  –  $2.0 \times 10^{-21}$  mg/mL). Tylosin-containing broth (5 mL) was then added to 5 mL of 1x Tris/ Glycine/ SDS buffer. A control was created using 5 mL of LB broth and 5 mL of buffer. *B. subtilis* (100 µL of 50 mg/mL stock solution) was



then added, and samples were incubated at 25°C for forty-eight hours. Initial cell growth was measured by monitoring  $A_{500}$  at eight, twelve, and twenty-four hours.

### **Section 2.3: Modified Bradford Assay:**

Total protein concentration of each homogenized sample was determined as follows. A Bradford Standard Albumin (BSA) curve was first obtained using a BSA standard ranging from 10-40 mg. To each BSA sample 10  $\mu$ L of 2-DE buffer, 10  $\mu$ L of 0.1 M HCl, and 80  $\mu$ L of glass-distilled water was added. The samples were mixed and 4 mL of Bradford dye reagent (Coomassie Blue G-250, 95% Ethanol, 85% o-Phosphoric Acid) was added. The *B. subtilis* samples consisted of 1-10  $\mu$ L of bacterial protein, 10  $\mu$ L of 0.1 M HCl, 80  $\mu$ L of glass-distilled water, and 4 mL of Bradford dye reagent. In a cuvette, Absorbance was measured at 595 nm in a UV-VIS Spectrophotometer against a blank of assay mixture without protein. The BSA curve was obtained by plotting absorbance versus BSA concentration. The concentration of the *B. subtilis* samples, treated and untreated, were determined using the equation of the line produced (1).

### **Section 2.4: Two-Dimensional Gel Electrophoresis:**

Bio-Rad Isoelectric Focusing (IEF) 7 cm strips of pH 3-10 were placed in a focusing tray and loaded with 100  $\mu$ g of protein and active rehydration buffer (8 M Urea, 2% CHAPS, 50 mM DTT, 0.2% Bio-Lyte 3110 Ampholyte, 0.001% Bromophenol Blue) to a final volume of 125  $\mu$ L per strip and overlaid with mineral oil. IEF strips were rehydrated for twelve hours at 50 mV. Strips were focused in a Bio-Rad Protean IEF Cell for 40,000 Vhr (4,000 v potential and linear ramp). IEF strips were removed and placed in equilibration buffer I (6 M Urea, 2% SDS, 0.375 M Tris-HCl pH 8.8, 20% Glycerol, 130

mM DTT) with shaking, via an orbital shaker, for thirty minutes followed by thirty minutes in equilibration buffer II (6 M Urea, 2% SDS, 0.375 M Tris-HCl pH 8.8, 20% Glycerol, 135 mM Iodoacetamide) (2).

IEF strips were laid on top of 17 cm 10% polyacrylamide gels (40% Acrylamide, 1.5 M Tris pH 8.8, glass-distilled water, 10% Ammonium Persulfate, 10% SDS, TEMED). Overlay agarose (0.5% Agarose in 1x Tris/ Glycine/ SDS buffer and 0.003% Bromophenol Blue) was layered overtop of the IEF strips and allowed to harden. The gels were placed in a mini-gel box and vertical electrophoresis commenced, with cooling, at 16mA per gel until the dye front reached the bottom. The gel was removed and stained as follows in Coomassie Brilliant Blue. The gel was separated from the glass plates and placed in enough stain to completely cover it. The gel is placed on an orbital shaker overnight followed by washings with low concentration water-methanol- acetic acid (84:10:6) destain solution. The gel was destained until all background dye was removed.

### **Section 2.5: Imaging:**

All destained gels are photographed and compared using PDQuest 2-D imaging software and camera. At least three gel images of treated and untreated *B. subtilis* samples at varying concentrations were used to create a match set. Each of the three images is compared to each other and similar/dissimilar protein spots are highlighted. From these results a master image is created representing results from all gels in the match set. Once a treated and untreated match set was completed, a higher lever (HL) match set was generated using the master gel images from each match set and protein spots were again compared for analysis (3).

## **Section 2.6: References:**

1. Ramagli, L.S.; Rodriguez, L.V. Quantitation of Microgram Amounts of Protein in Two-Dimensional Polyacrylamide Gel Electrophoresis Sample Buffer. *Electrophoresis*. **1985**, 6, 559-563.
2. Bio-Rad. *ReadyStrip IPG Strip Instruction Manual*; Bio-Rad Laboratories: California, 2002.
3. *PD Quest 2-D Analysis Software*, Version 7.1; Bio-Rad Laboratories: California, 2002.

## **Chapter 3**

### Results and Discussion

### **Section 3.1: Results of MIC Determination:**

Absorbance at 500 nm was measured for six Tylosin-treated *B. subtilis* test samples that were serially diluted from concentrations ranging from  $2.0 \times 10^{-6}$  –  $2.0 \times 10^{-21}$  mg/mL at time points of eight, twelve, and twenty-four hours. A control sample of *B. subtilis* without Tylosin was maintained in identical conditions to monitor normal bacterial growth.

A dosage curve (figure 3.1) was created using the absorbance readings for the eight, twelve, and twenty-four hour time points and the known concentrations of Tylosin in each treated sample. From the graph and data collected, it is apparent that the minimum inhibitory concentration would be  $2.0 \times 10^{-9}$  mg/ml. This would appear to be the lowest concentration where *B. subtilis* was inhibited the most before the increase in growth at ineffective concentrations.

### **Section 3.2: Results of the Modified Bradford Assays:**

Two modified Bradford assays were performed on a total of six *B. subtilis* treated and untreated samples in order to calculate the total protein concentration in each sample. From the resulting equation from the graph (figure 3.2), the protein concentrations of treated sample 4.01 mg/ml and untreated sample 5.84 mg/ml were calculated. The second BSA standard curve, similar to methods above, the protein concentrations of untreated samples 5.73 mg/ml and 6.94 mg/ml along with treated samples 9.12 mg/ml and 12.61 mg/ml were determined via figure 3.3.

### **Section 3.3: Results of the Treated Match Set:**

The treated match set was constructed based on the gel image featured in figure 3.4. This is an uncropped gel representation of protein sample (4.01 mg/ml). This gel displayed the protein expression profile of what is expected in Tylosin-treated *B. subtilis* protein samples. A pH scale ranging from 3-10 was inserted on top of the gel image to better illustrate the regions of protein separation by IEF. From this image a box was drawn to enclose four protein spots arranged diagonally that became spots of interest. These four protein spots, located in the neutral to weakly basic pH range of 7.0-8.0 were profiled in this proteomic study. These spots were chosen because they are easily located, dark in color and large in size.

The complete treated match set, figure 3.5, featuring Tylosin-treated *B. subtilis* protein sample concentrations of 4.01 mg/ml, 9.12 mg/ml, and 12.61 mg/ml were cropped to be the same size. The four protein spots of interest were boxed on each individual gel image. These same spots can be seen on a created Gaussian master gel image, reinforcing that these spots are prevalent to all the gels in the treated match set.

Using Bio-Rad image software analysis, comparisons were made between the gel images in the treated match set and the master gel image generated. In figure 3.6, the green highlighted protein spots were found to be in common with all gel images, while those in red were unmatched. Table 3.1 shows a summary of protein spot analysis within the Tylosin-treated *B. subtilis* match set. All gel images have at least four spots of interest in common. The treated protein sample of 4.01 mg/ml has a 100% spot comparison since it was the template gel used to create the master gel image.

### **Section 3.4: Results of the Untreated Match Set:**

An untreated match set was constructed based on the gel image in figure 3.7. This is an uncropped gel representation of protein sample 5.73 mg/ml. The gel displayed the protein expression profile of what is expected by *B. subtilis* protein samples. Again, a pH scale ranging from 3-10 was inserted on top of the gel image to better illustrate the regions of protein separation by IEF. From this image a box was drawn to enclose the same four diagonal protein spots, as seen in the treated gel images. These four protein spots were still located in the neutral to weakly basic pH range of 7.0-8.0 and are consistent with what was seen in the treated gel images.

The complete untreated match set, figure 3.8, featuring *B. subtilis* protein sample concentrations of 5.73 mg/ml, 5.84 mg/ml, and 6.94 mg/ml were cropped to be the same size. The four protein spots of interest were boxed on each individual gel image. These same spots can be seen on a created Gaussian master gel image, reinforcing that these spots are prevalent to all the gels in the treated match set.

Using Bio-Rad image software analysis, comparisons were made between the gel images in the untreated match set and the master gel image generated. In figure 3.9, the green highlighted protein spots were found to be in common with all gel images, while those in red went unmatched. Table 3.2 shows a summary of protein spot analysis within the *B. subtilis* match set. All gel images have at least twelve spots of interest in common. The untreated protein sample of 5.84 mg/ml has a 100% spot comparison since it was the template gel used to create the master gel image.

### **Section 3.5: Results of the Higher Level Match Set:**

A higher level match set (figure 3.10) featuring the master gel images of the treated and untreated match sets were created using Bio-Rad Imaging software. Once again the four protein spots of interest are present and isolated within a box. A master gel image was generated using the untreated master gel image as a template.

The comparison of the two match sets can be seen in figure 3.11. The untreated master gel image has a spot comparison of 100% and is the only gel used in the creation of the higher level master image. This is because the treated master gel image does not match the untreated master image by computational methods. However the spots of interest, designated by the box, appear to be similar and those spots in the treated sample are shifted slightly downward and to the left to a more neutral pH region.

### **Section 3.6: Discussion:**

The purpose of this study was to compare and contrast the protein expression profile of the ATCC 6051-T strain of *B. subtilis* with a corresponding Tylosin-treated protein expression profile of the bacteria. In determining the approximate drug concentration to apply as an MIC, the data (figure 3.1) used to choose this number,  $2.0 \times 10^{-9}$  mg/ml, was within the macrolide limit. Prior research by Noli and Boothe determined that organisms are susceptible to macrolides at an MIC of less than 2 mg/ml (1).

The individual protein concentrations desired by the modified Bradford assay fall between the ranges of 1-5 mg/ml, with most protein concentrations exceeding this, which made for healthy protein samples fit for two-dimensional analysis.



In analysis of the 2-DE gels of the untreated versus treated match sets, it is important to notice that the two protein expression profiles have very few similarities. The untreated match set (figure 3.8) demonstrates a clear dispersion of individual proteins. These protein spots are very dark in color indicating a significant protein concentration for more than half of the spots visible by imaging. *B. subtilis* is plentiful when allowed to grow without inhibition as is seen by protein spot quantity. Whereas visually observing the treated match set (figure 3.5), featuring the antibiotic Tylosin, protein analysis was limited. The protein spot expression profile generated in the treated match set is less intense than those proteins seen in the untreated match set. This means that visualization was poor due to faded or even smeared spots attributable to a lower protein concentration per spot. Only about one-third of the original total protein number, seen in the untreated match set, was recovered in the treated match set, which expressed the efficiency of Tylosin on the growth of *B. subtilis*.

The only similarity that can be drawn between the two match sets was the four diagonally placed protein spots, designated inside a box. These four protein spots are similar in size when compared to both match sets but spot intensity is decreased in the treated match set as would be expected in growth with a protein synthesis inhibitor such as an antibiotic.

In statistical comparison of the two match sets (figure 3.11), again no direct spot comparisons can be made via computational methods. In two-dimensional software analysis, several spot centers were identified in the 5.84 mg/ml gel image used as the master in the untreated match set. These spot centers were used to identify protein matches among each gel image used in the untreated match set (figure 3.9). This was

quite successful in generating protein matches as was summarized in table 3.2 with at least twelve spots in common per gel image. Only four spots were identified as being similar in the treated match set (table 3.1) and the image analysis of the data (figure 3.6) confirmed this. What was discovered was that the four spots identified on the treated match set correspond to the four spots of interest examined in this study. These four spots have also been identified in the untreated match set as well. The main visual difference in the comparison of the four “boxed” protein spots was that their placement in the treated match set was noticed to be the subtle downward shift to the left. This shift still kept the four protein spots inside the designated pH range of 7.0-8.0, but they are not at their original location.

A plausible reason for this result could be inhibition of the enzyme peptide deformylase (PDF) in the elongation phase of protein synthesis. It is here that the formyl group can be removed.

Apfel and his group studied the Gram-positive bacteria *Haemophilus Influenza* and *Streptococcus pneumoniae* with PDF inhibitor actinonin. Numerous spot shifts were observed after treatment with inhibitor (figure 1.7) indicating a decrease in isoelectric points of all shifted proteins. Their assumption was that the shifts were a result of the formyl groups that were not removed and consequently blocked the N-terminal amino group. Little change was observed for high molecular weight proteins. This at least correlates with the Tylosin-treated gel image. The four spots of interest would be considered in a low molecular weight range as well (2).

Another published study, done by Bandow, supports the claim of PDF inhibition. Here wild-type *B. subtilis* was subjected to growth with actinonin. Their protein map of

the bacteria also showed that the majority of cytoplasmic proteins shifted toward a more acidic pI. Figure 1.6 isolated the shifting of one protein spot in their theoretical map created (3).

Tylosin, belonging to the macrolide class of antibiotics, would exert its powers of inhibition on the 50S subunit, containing the peptidyl transferase center which catalyzes the formation of peptide bonds by binding close to this center (4). Based on prior studies and the results of this one here, it would appear that the mystery of pI shifting might have something to do with extension of new polypeptides. Although the only sure way to prove this hypothesis and validate the reasoning behind it would be to sequence the available proteins spots and compare the similarities.

### **Section 3.7: References:**

- (1). Noli, C.; Boothe, D.; Macrolides and Licosamides. *Veterinary Dermatology*. **1999**, 10, 217-223.
- (2). Apfel, C.; Locher, H.; Evers, S.; etc. Peptide Deformylase as an Antibacterial Drug Target: Target Validation and Resistance Development. *Antimicrob. Agents Chemother.* **2001**, 45, 1058-1064.
- (3). Bandow, J.; Hecker, M.; Labischinski, H.; etc. Proteomic Approach to Understanding Antibiotic Action. *Antimicrob. Agents Chemother.* **2003**, 47, 948-955.
- (4). Douthwaite, S. Structure Activity Relationships of Ketolides vs. Macrolides. *CMI*. **2001**, 7, 11-17.

**Figure 3.1**

Growth Curve of *Bacillus subtilis* with Tylosin

## B. subtilis Growth with Tylosin

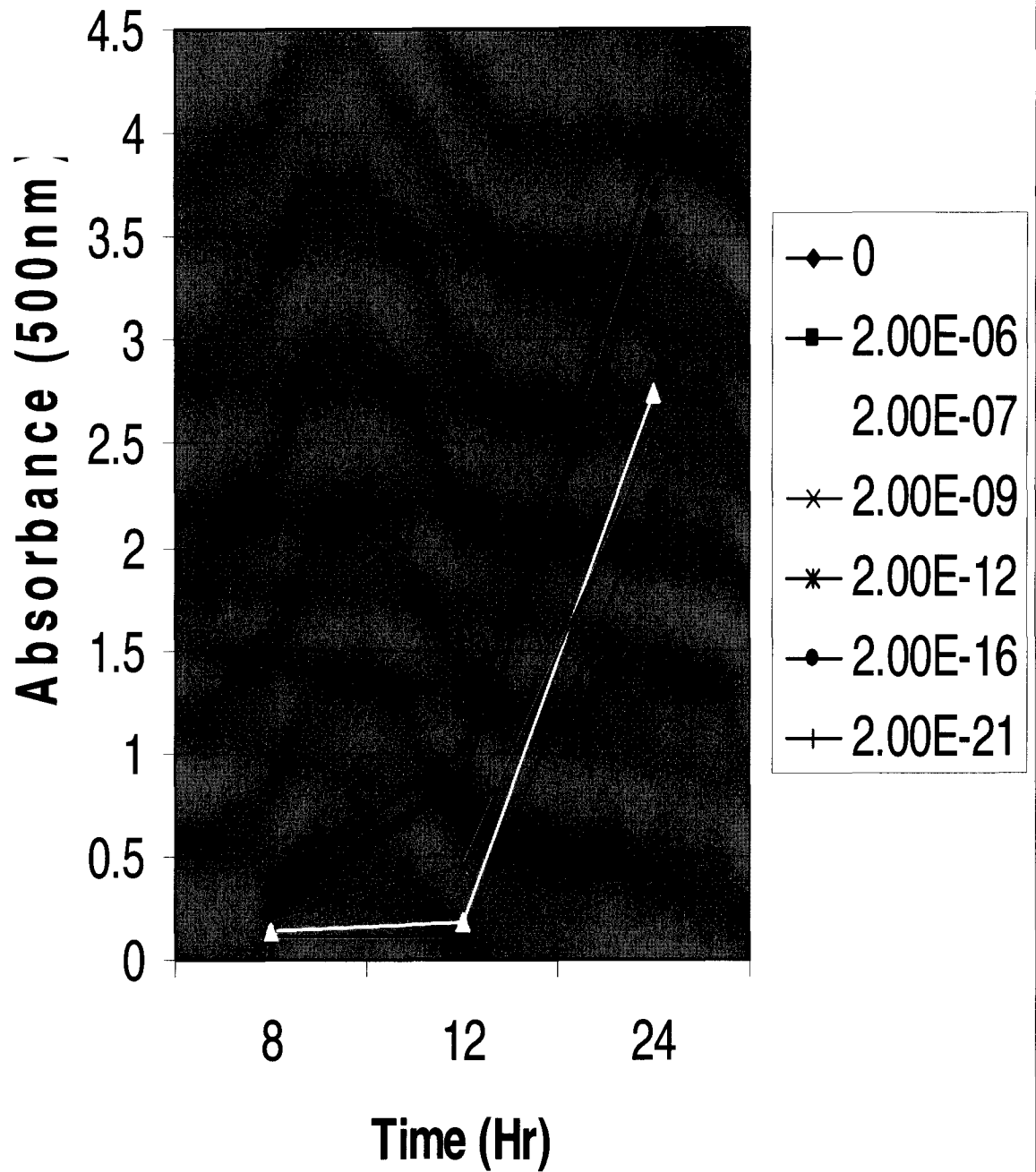


**Figure 3.2**

Absorbance vs. Concentration for *Bacillus subtilis* 5.84 mg/mL and Tylosin-Treated  
*Bacillus subtilis* 4.01 mg/mL Protein Samples

# modified bradford assay

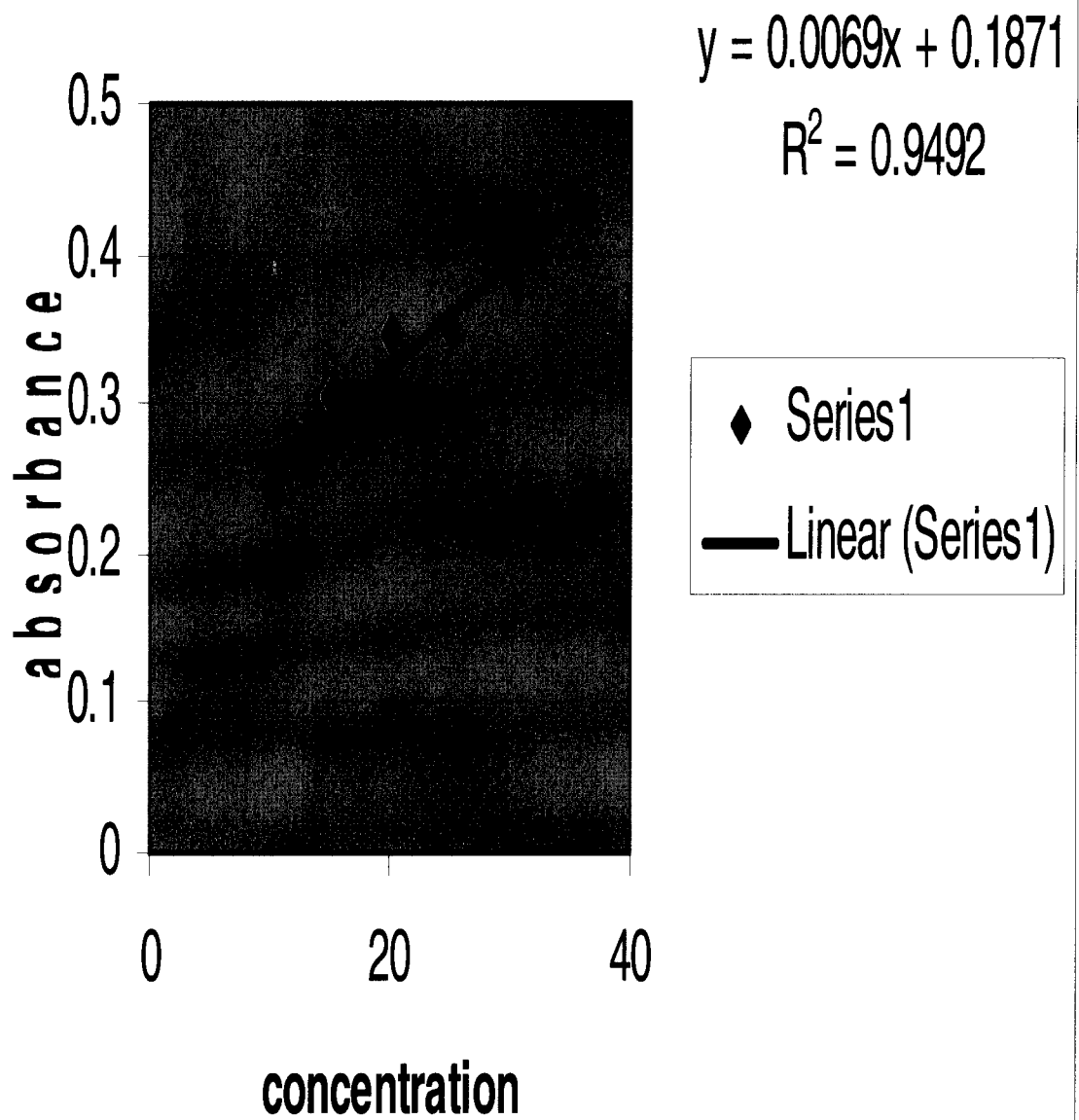




**Figure 3.3**

Absorbance vs. Concentration for *Bacillus subtilis* 5.73 mg/mL, 6.94 mg/mL and Tylosin-Treated *Bacillus subtilis* 9.12 mg/mL, 12.61 mg/mL Protein Samples

## modified bradford assay

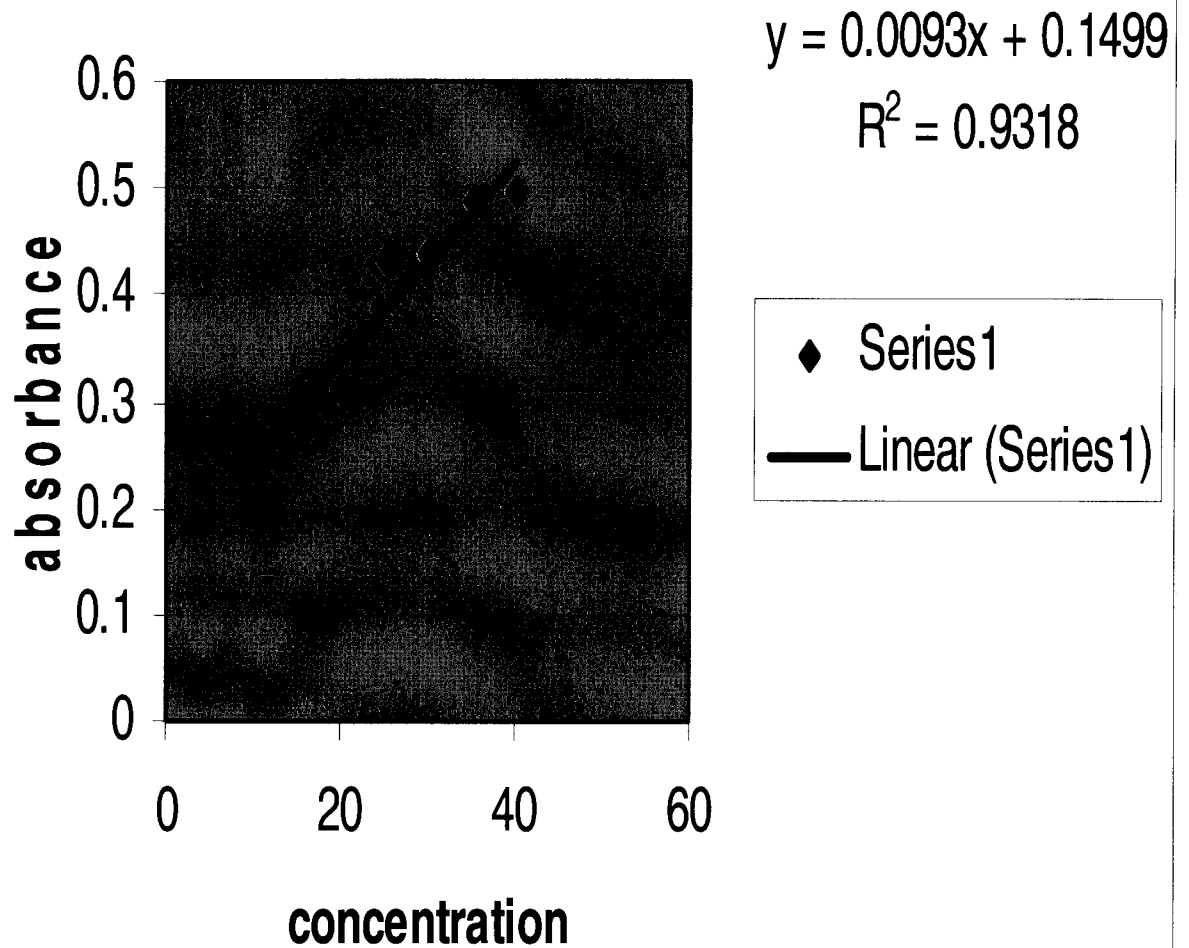


**Figure 3.4**

Tylosin-Treated *Bacillus subtilis* uncropped 4.01 mg/mL Gel Image

3

4

5

6

7

8

9

10

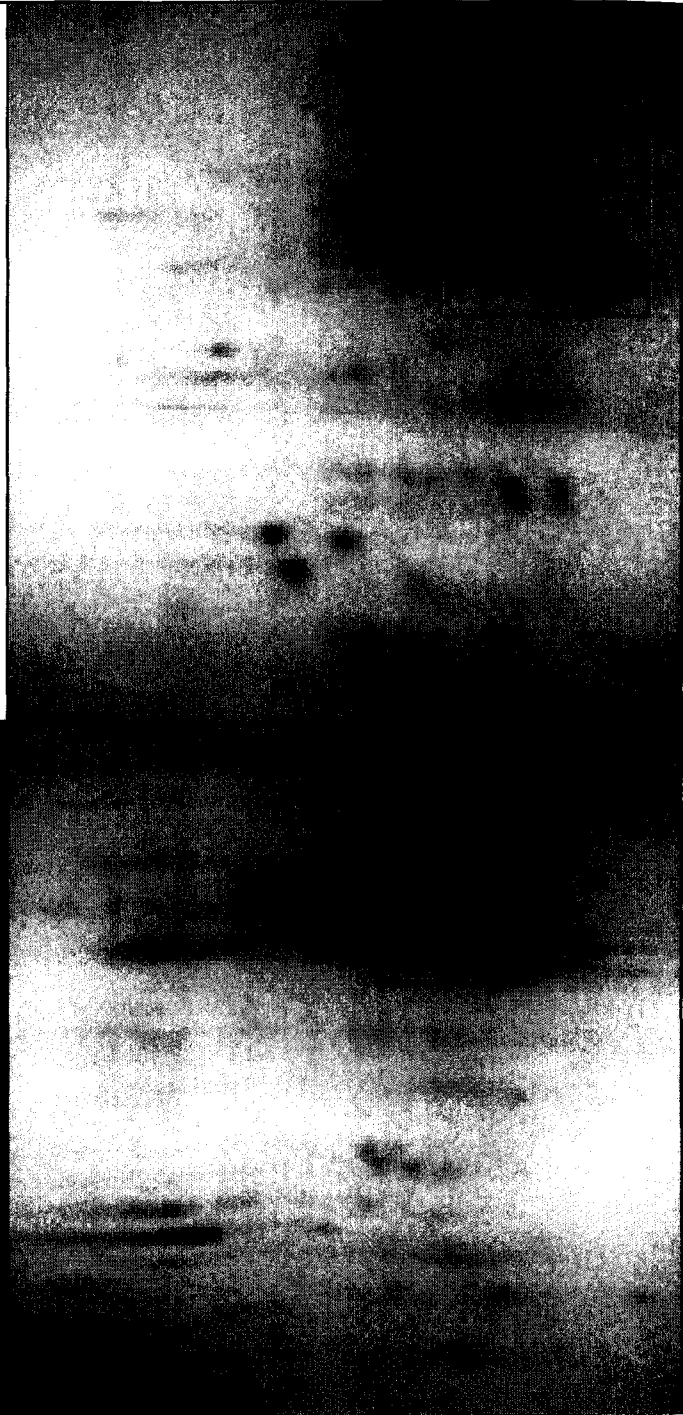
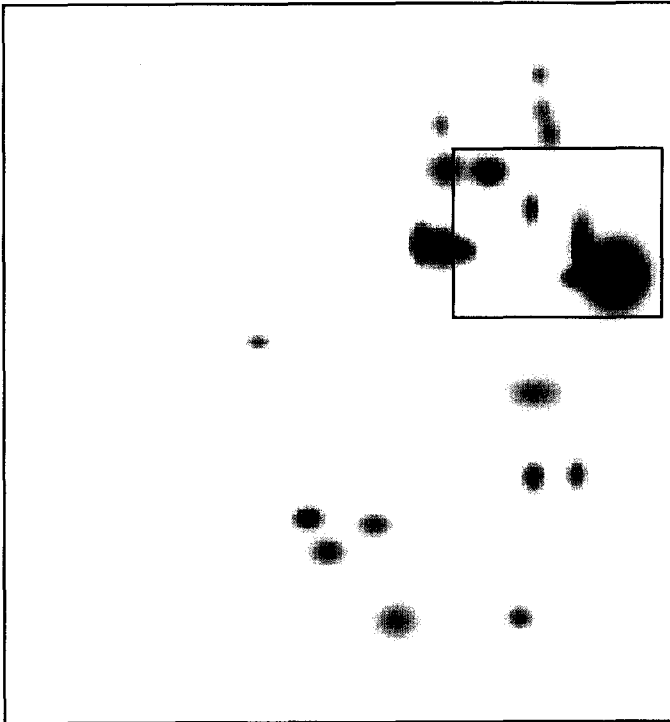


**Figure 3.5**

Tylosin-Treated *Bacillus subtilis* Match Set

Tylosin-Treated Master Gel

Tylosin-Treated 4.01 mg/mL Gel



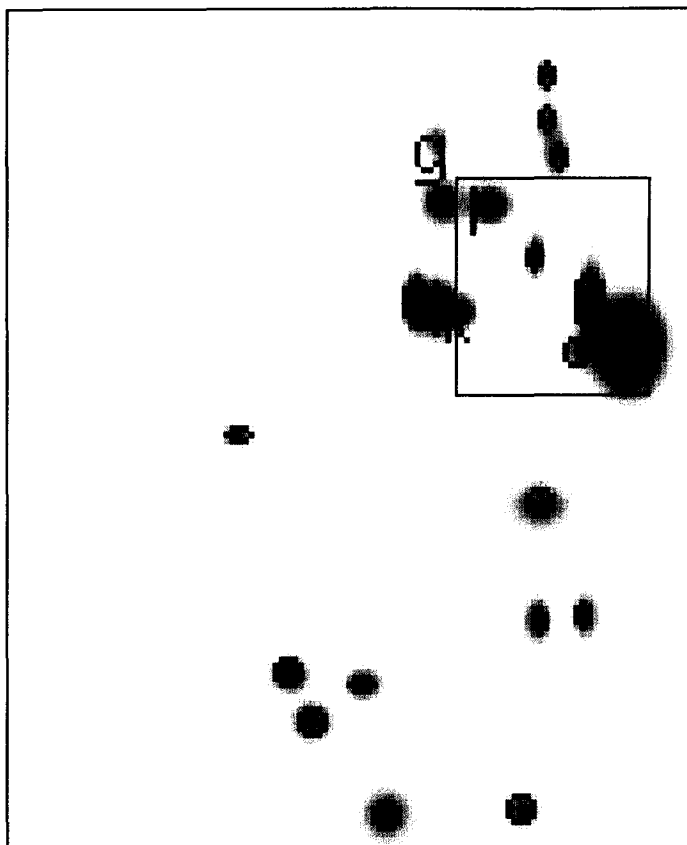
Tylosin-Treated 9.12 mg/mL Gel

Tylosin-Treated 12.61 mg/mL Gel

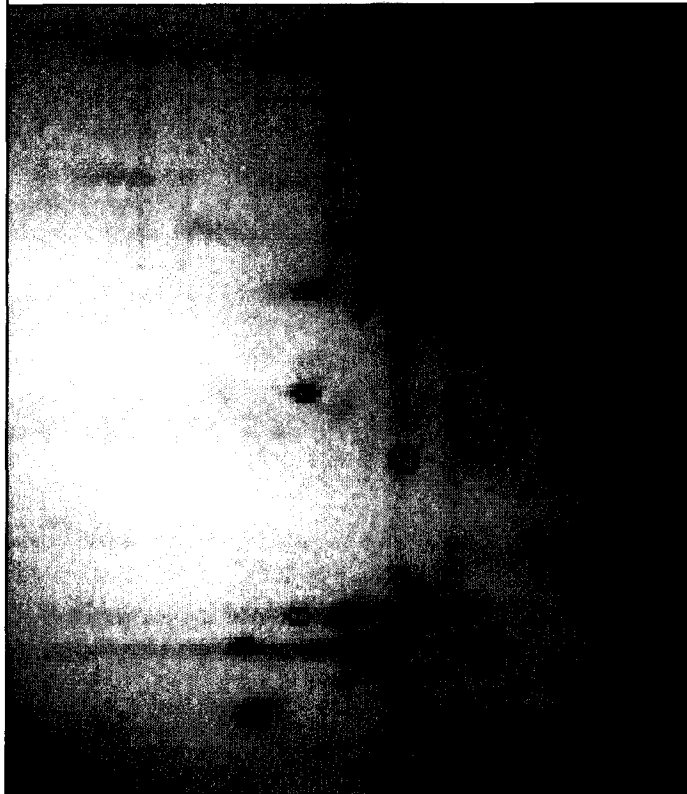
**Figure 3.6**

Tylosin-Treated *Bacillus subtilis* Match Set with Protein Spot Comparisons

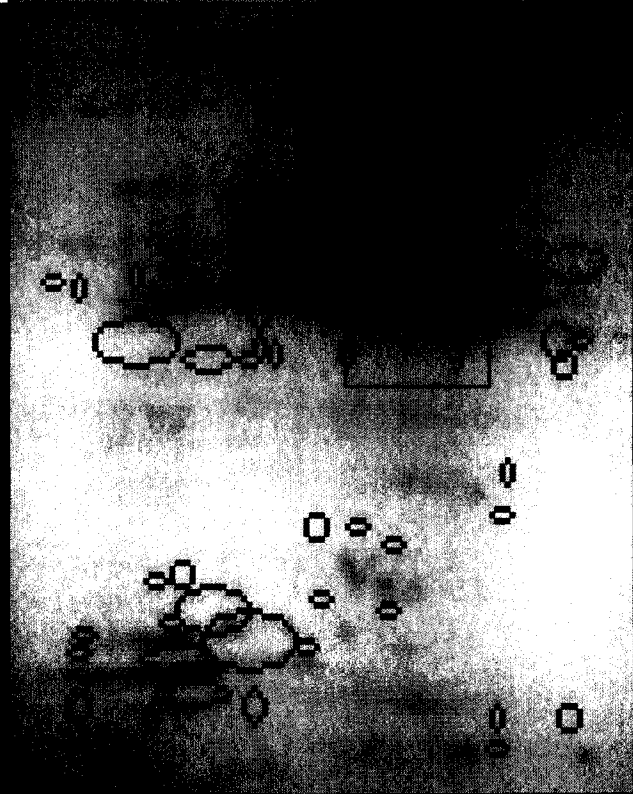
Tylosin-Treated Master Gel



Tylosin-Treated 4.01 mg/mL Gel



Tylosin-Treated 9.12 mg/mL Gel



Tylosin-Treated 12.61 mg/mL Gel



**Table 3.1**

Summary of Tylosin-Treated Match Set

<b>Gel Image</b>	<b>Matched Spots</b>	<b>Unmatched Spots</b>	<b>Percentage (%)</b>
Master Gel	4	18	22
9.12 mg/mL	4	33	12
12.61 mg/mL	4	66	6
4.01 mg/mL	22	0	100

**Figure 3.7**

Untreated *Bacillus subtilis* uncropped 5.73 mg/mL Gel Image

3

4

5

6

7

8

9

10

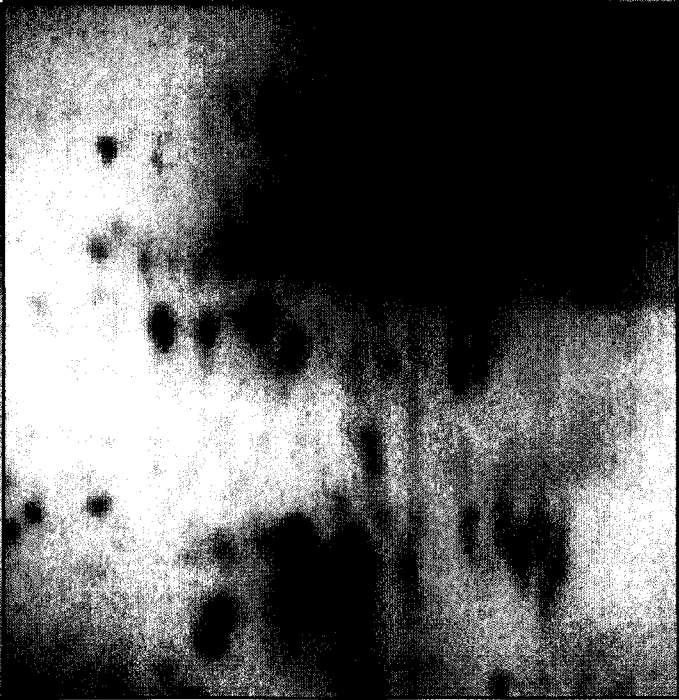
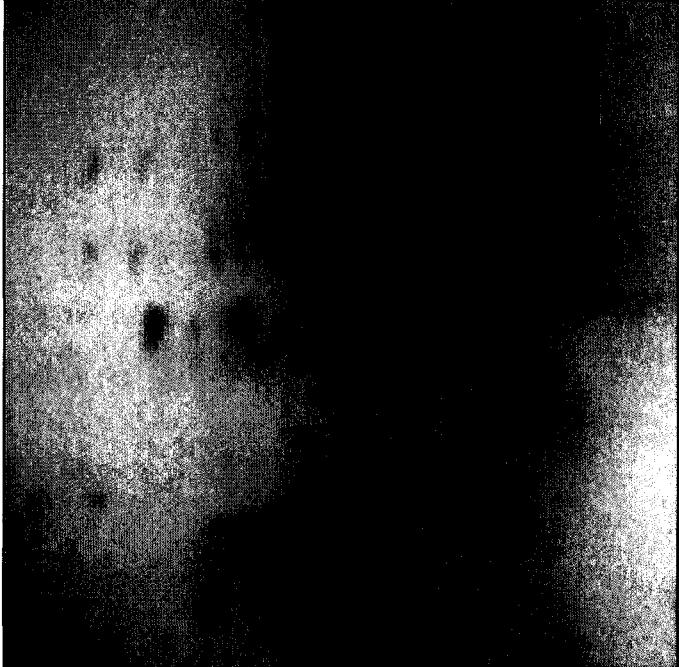
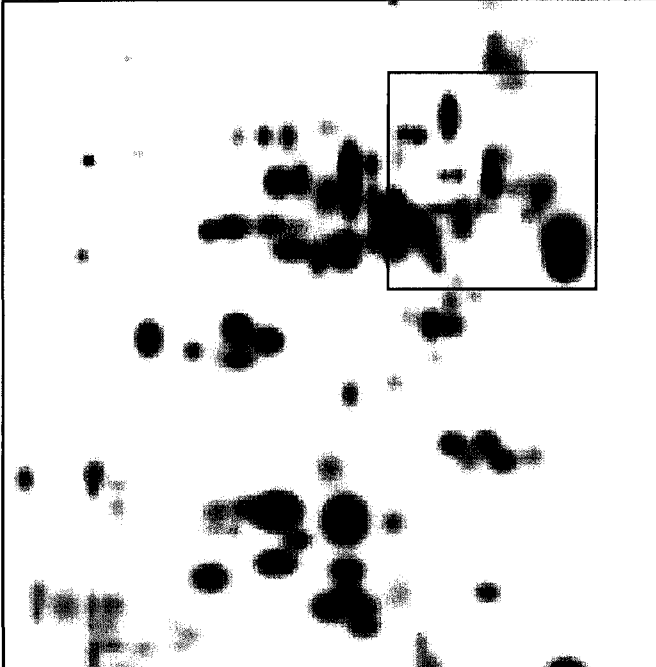


**Figure 3.8**

Untreated *Bacillus subtilis* Match Set

Untreated Master Gel

Untreated 5.73 mg/mL



Untreated 5.84 mg/mL Gel

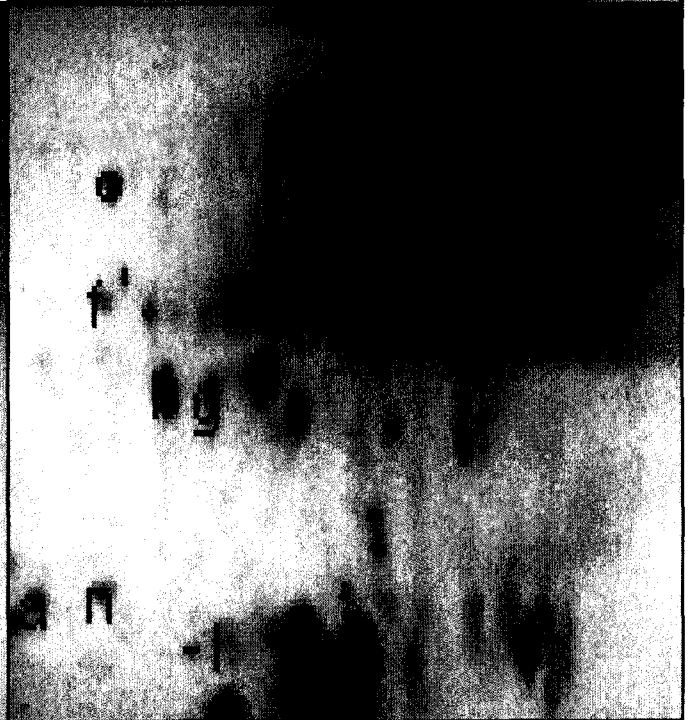
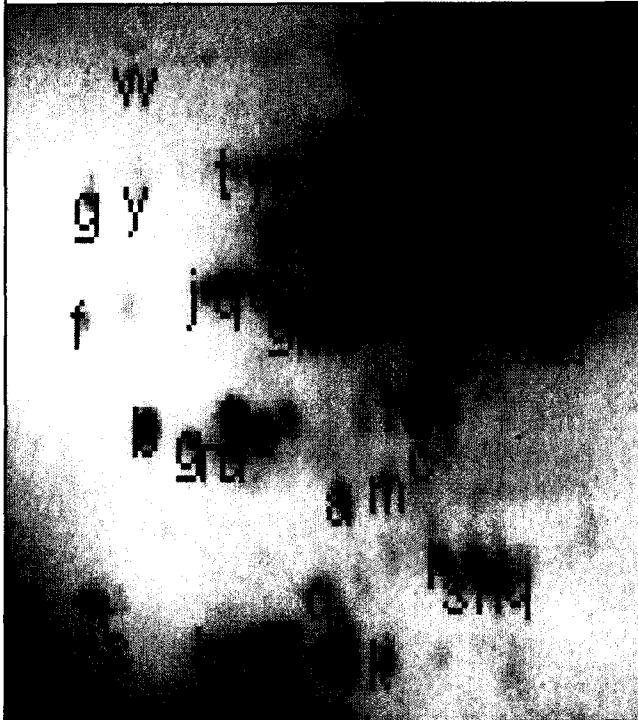
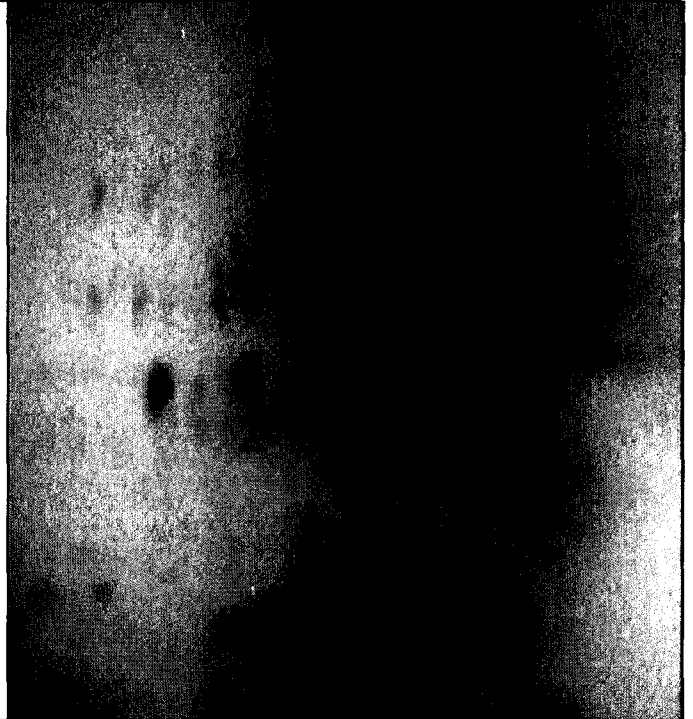
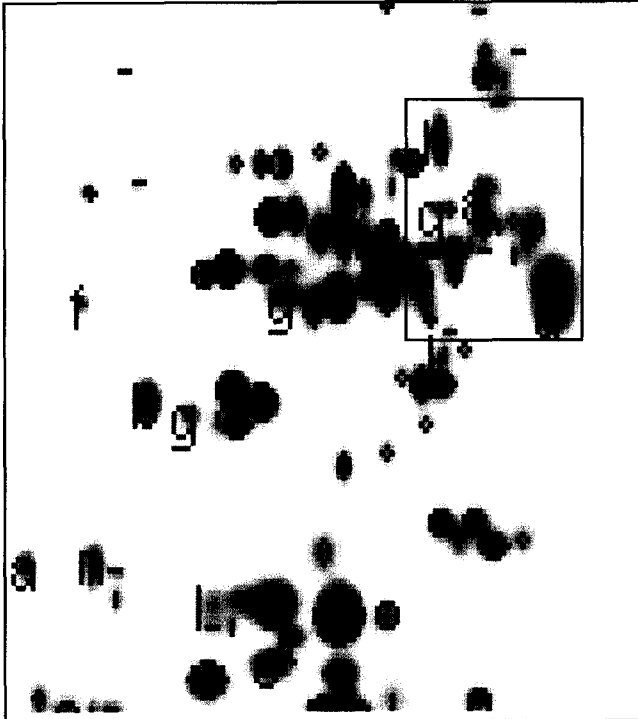
Untreated 6.94 mg/mL Gel

**Figure 3.9**

Untreated *Bacillus subtilis* Match Set with Protein Spot Comparisons

Untreated Master Gel

Untreated 5.73 mg/mL Gel



Untreated 5.84 mg/mL Gel

Untreated 6.94 mg/mL Gel



**Table 3.2**

Untreated *Bacillus subtilis* Match Set Summary

<b>Gel Image</b>	<b>Matched Spots</b>	<b>Unmatched Spots</b>	<b>Percentage (%)</b>
Master Gel	20	115	17
5.73 mg/mL	12	60	20
6.94 mg/mL	20	57	35
5.84 mg/mL	135	0	100

**Figure 3.10**

Higher Level Match Set Featuring the Master Gel Images of the Treated and Untreated

*Bacillus subtilis* Match Set

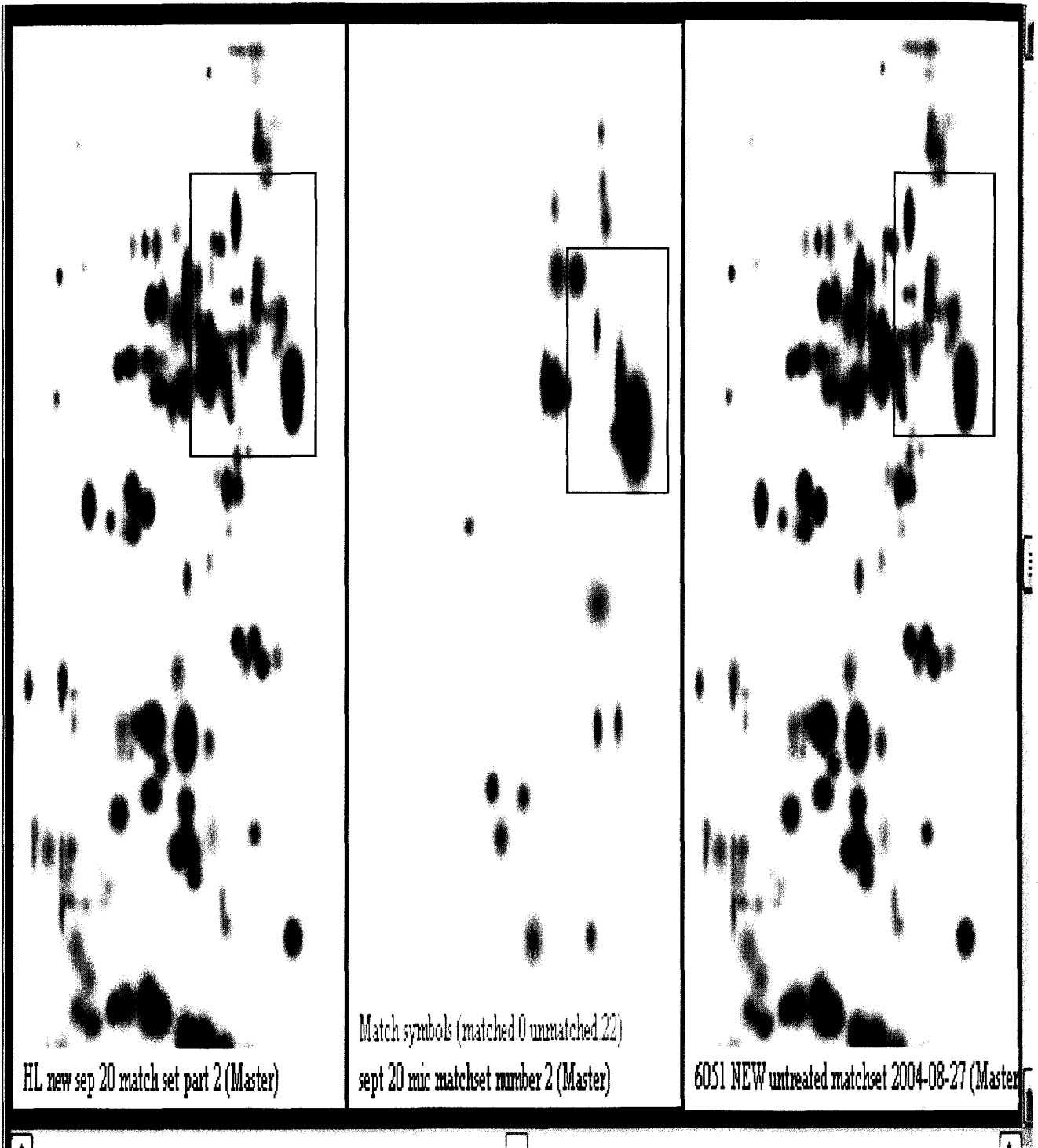
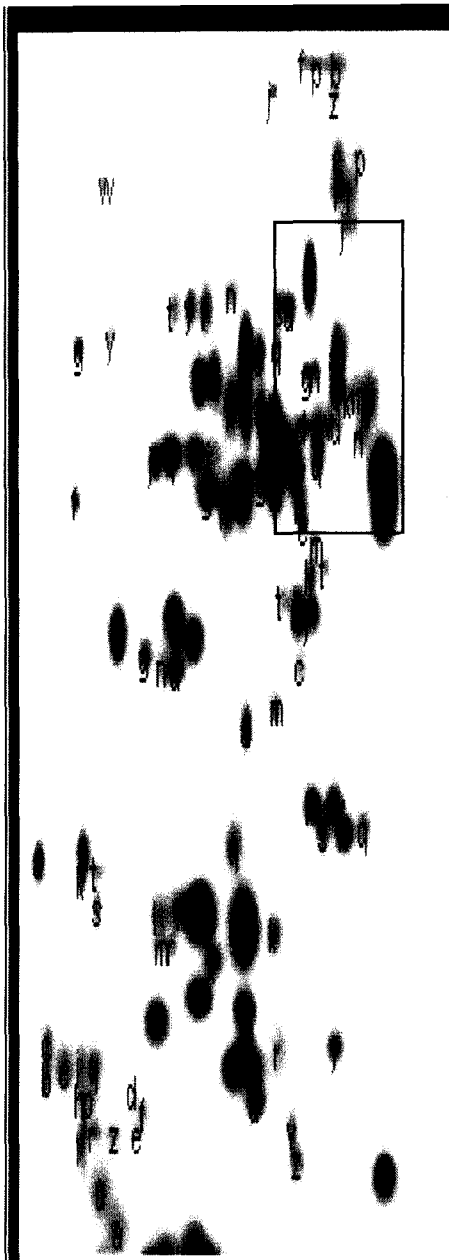
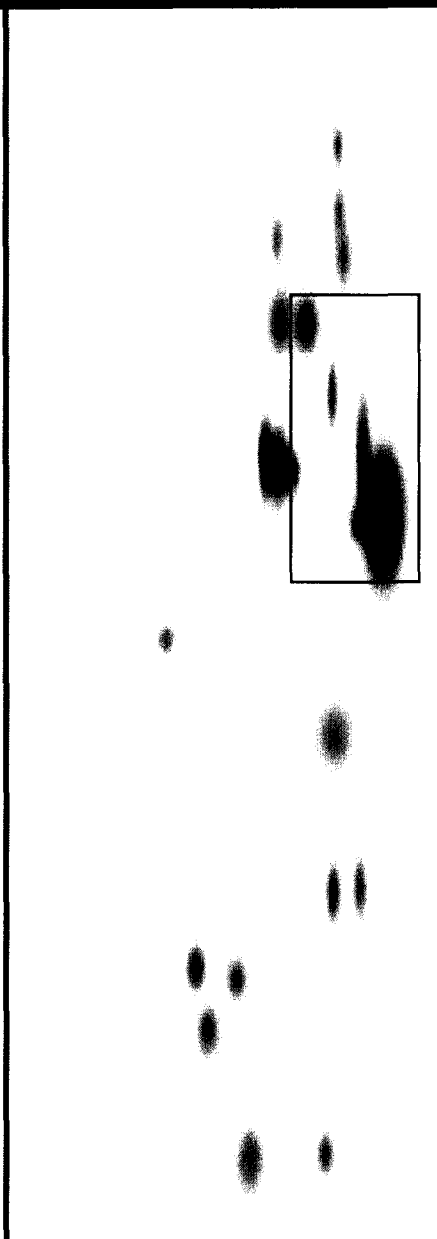


**Figure 3.11**

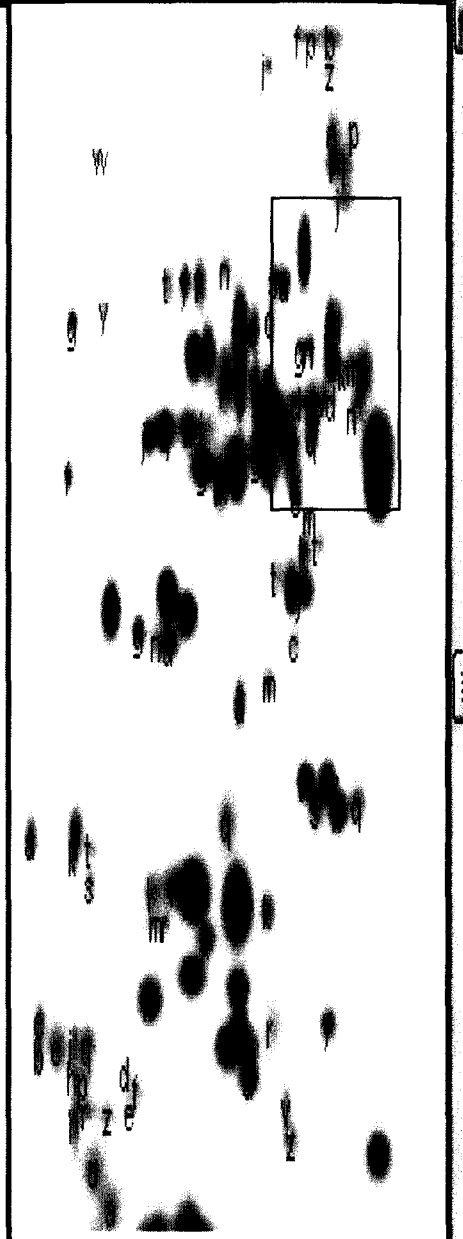
Higher Level Match Set with Protein Spot Comparisons



Match symbols (matched:135 unmatched:0)  
 HL<sup>Q</sup> new sep 20 match set part 2 (Master)



Match symbols (matched:0 unmatched:22)  
 sept 20 mic matchset number 2 (Master)



Match symbols (matched:135 unmatched:0)  
 6051 NEW untreated matchset 2004-08-27 (Master)

## **Appendix I**

Solutions Needed for Experiments

### **Recipes:**

*TE Buffer pH 7.5:* combine 0.6057 g of 10 mM tris with 0.18612 g of 1 mM EDTA and dilute to 500 mL.

*Bradford Dye:* Dissolve 100 mg of Coomassie brilliant blue G-250 in 50 mL of 95% ethanol. Add 100 mL of 85% o-phosphoric acid; dilute to 1 L and filter.

*1x Tris / Glycine / SDS Buffer:* Combine 3.02 g of 25 mM tris, 14.41 g of 192 mM glycine , and 0.1 g of 0.1% SDS; dilute to 1 L.

*Equilibration Buffer I:* Combine 3.6 g of 6 M urea, 0.2 g of 1% SDS, 2.5 mL of tris-HCL buffer pH 8.8, 2.0 mL of 20% glycerol, and 200 mg of 130 mM DTT; dilute to 10 mL.

*Equilibration Buffer II:* Same as equilibration buffer I, but omit DTT and add 250 mg of 135 mM iodoacetamide.

*Active Rehydration Buffer:* Combine 50  $\mu$ L of 0.2% bio-lyte 3110 ampholyte, 4.819 g of 8 M urea, 0.106 g of 2% CHAPS, 0.027 g of 50 mM DTT; dilute to 10 mL.

*Luria-Bertani Broth:* Combine 5.00 g of bacto tryptone, 2.50 g of bacto yeast extract, and 5.00 g of sodium chloride; dilute to 500 mL and autoclave.

*2DE Buffer:* Combine 25.27 g of 8.4 M urea, 9.15 g of 2.4 M thiourea, 2.54 g of 5% CHAPS, 0.39 g of 50 mM DTT, and 2.50 mL of 25 mM spermine base; dilute to 1 L.